FINITE ELEMENT ANALYSIS OF BENDING OPERATION OF ALUMINUM PROFILES

A THESIS SUBMITTED TO
THE GRADUATE SCHOOL OF NATURAL AND APPLIED SCIENCES
OF
MIDDLE EAST TECHNICAL UNIVERSITY

BY

UFUK PENEKLİ

IN PARTIAL FULFILLMENT OF THE REQUIREMENTS
FOR
THE DEGREE OF MASTER OF SCIENCE
IN
MECHANICAL ENGINEERING

APRIL 2008

Approval of the thesis:

FINITE ELEMENT ANALYSIS OF BENDING OPERATION OF ALUMINUM PROFILES

submitted by **UFUK PENEKLİ** in partial fulfillment of the requirements for the degree of **Master of Science in Mechanical Engineering Department, Middle East Technical University** by,

Prof. Dr. Canan Özgen _________________
Dean, Graduate School of **Natural and Applied Sciences**

Prof. Dr. S.Kemal İder _________________
Head of Department, **Mechanical Engineering**

Prof. Dr. Haluk Darendeliler
Supervisor, **Mechanical Engineering Dept., METU** _________________

Prof. Dr. Süha Oral
Co-Supervisor, **Mechanical Engineering Dept., METU** _________________

Examining Committee Members:

Prof. Dr. Kemal İder, _________________
Mechanical Engineering Dept., METU

Prof. Dr. Haluk Darendeliler, _________________
Mechanical Engineering Dept., METU

Prof. Dr. Süha Oral, _________________
Mechanical Engineering Dept., METU

Assist. Prof. Yiğit Yazıcıoğlu _________________
Mechanical Engineering Dept., METU

Prof. Dr. Can Çoğun _________________
Mechanical Engineering Dept., Gazi University

Date: 04 – 15 – 2008

I hereby declare that all information in this document has been obtained and presented in accordance with academic rules and ethical conduct. I also declare that, as required by these rules and conduct, I have fully cited and referenced all material and results that are not original to this work.

Name : Ufuk PENEKLİ

Signature :

ABSTRACT

FINITE ELEMENT ANALYSIS OF BENDING OPERATION OF ALUMINUM PROFILES

Penekli, Ufuk

M.S., Department of Mechanical Engineering

Supervisor : Prof. Dr. Haluk Darendeliler

Co-Supervisor : Prof. Dr. Süha Oral

April 2008, 85 pages

Bending process is an important forming process in most industrial fields. Springback and cross-section distortion are commonly faced problems in bending process. Springback behavior of closed and open section beams changes with different parameters such as cross-section type, cross-section dimensions, bend radius and bend angle. For closed sections like tube, the dominating problem is cross-section distortion. The thickness of the tube at intrados (inner surface of tube being in contact with die) increases, whereas the thickness of the tube at extrados (outer surface of tube) decreases. Furthermore, another cross-section distortion type for tubes is flattening at extrados which is undesirable in some manufacturing operations.

The present research, using finite element method, focuses on investigating the springback behavior of commonly used aluminum beams which are T-Shaped, U-Shaped and tubular for different cases. A series of analyses is performed for a beam and the changing parameters in the analyses are bend radius and thickness.

Furthermore, for tubes, the effects of axial force on springback behavior are investigated. It is seen that the axial force causes stretching and the springback angles are decreased.

Moreover, in order to overcome cross-section distortion in flattening for tubes, different internal pressures are used and the effects of internal pressure are investigated. By applying appropriate internal pressure, the flattening distortion is mostly eliminated.

Conclusions are drawn revealing springback behaviors and cross-section distortions with respect to bend radius, bend angle, thickness, axial pull and internal pressures. They are in good agreement with other published researches and experimental results. Therefore, the models can be used to evaluate tooling and process design in bending operations.

Keywords: Rotary Draw Bending, Finite Element Method, Springback, Cross-Section Distortion.

ÖZ

ALUMİNYUM PROFİLLERİN BÜKÜM İŞLEMİNİN SONLU ELEMANLAR ANALİZİ

Penekli, Ufuk
Yüksek Lisans, Makina Mühendisliği Bölümü
Tez Yöneticisi : Prof. Dr. Haluk Darendeliler
Ortak Tez Yöneticisi: Prof. Dr. Süha Oral

Nisan 2008, 85 sayfa

Bükme işlemi pek çok endüstri alanındaki en önemli metal şekillendirme operasyonlarından biridir. Bükme işlemi esnasında, insanlar genellikle geri yaylanma ve kesit alanındaki bozukluklar gibi problemlerle karşılaşmaktadırlar. Açık ve kapalı kesit alanına sahip profillerin geri yaylanma davranışları kesit alanlarının şekline, kesit alanı ölçülerine, bükme yarıçapına ve bükme açısına göre değişkenlikler gösterir. Boru gibi kapalı kesit alanına sahip profillerde sıklıkla karşılaşılan problem ise kesit alanındaki bozukluklardır. Borunun iç yüzeyinde (borunun kalıba değdiği yüzey) kalınlaşma görülürken, borunun dış yüzeyinde ise incelemelere rastlanır. Ayrıca, bu tarz profillerde karşılaşılan diğer bir problem ise de, bazı üretim operasyonlarında arzulanmayan, borunun dış yüzeyinde meydana gelen düzleşmelerdir.

Bu çalışmada, sonlu eleman yöntemi kullanılarak, sıklıkla kullanılan T-şeklinde, U-şeklinde ve boru şeklindeki alüminyum profillerin farklı durumlar için geri yaylanma davranışları ve kesit alanlarındaki bozukluklar incelenmiştir. Profiller için bir dizi analiz gerçekleştirilmiştir ve bu analizlerdeki değişkenler bükme yarıçapı, kalınlık olarak belirlenmiştir.

Ayrıca, borular için eksenel uygulanan kuvvetin profil üzerindeki geri yaylanmaya olan etkileri incelenmiştir. Görüldü ki, uygulanan eksenel kuvvet profil üzerinde gerdirmeye yol açmıştır ve neticesinde geri yaylanma açılarında düşüş meydana gelmiştir.

Bunlara ek olarak, borularda meydana gelen kesit alanındaki düzleşme problemini ortadan kaldırabilmek için farklı iç basınçlar uygulanmıştır ve iç basıncın etkileri incelenmiştir. Uygun iç basınç uygulandığı takdirde, borulardaki düzleşme problemi büyük ölçüde ortadan kaldırılmıştır.

Bükme yarıçapına, bükme açısına, kalınlığa, eksenel kuvvete ve iç basınca göre geri yaylanma ve kesit alanındaki bozukluklar için sonuçlar hazırlanmıştır. Sonuçlar, yayınlanan diğer araştırma sonuçlarıyla ve deneysel sonuçlarla tutarlılık göstermektedir. Böylelikle hazırlanan modeller, bükme operasyonlarındaki kalıp ve ürün tasarımlarında kullanılabilir.

Anahtar Kelimeler: Gerdirmeli Bükme, Sonlu Elemanlar Metodu, Geri Yaylanma, Kesit Alanı Bozuklukları.

To My Family

ACKNOWLEDGEMENTS

I would like to express my appreciation and thankfulness to Prof. Dr. Haluk Darendeliler for his encouragement and support that created this study.

I would like to thank Prof. Süha Oral for his kind help and support.

I also want to thank Prof.Dr. Kemal İder, Asst. Prof. Yiğit Yazıcıoğlu and Prof.Dr. Can Çoğun for their comments.

I owe Pınar Kaya for her precious help, support and friendship.

I would like to thank Koray Demir, for his invaluable collaboration and friendship.

Thanks to all my colleagues in FİGES, leading Emre Karalarlı, Murat Halisçelik and my manager Hakan Oka.

I would like to thank Emre Saçan, Onur Miskbay for being my friends; and the thanks extend to Günay Orbay.

The special thanks go to my parents Mücahit Penekli and Fevziye Penekli for their infinite support, and to my brothers Okan Penekli, Recai Penekli and sister Dilek B.Gölcigezli.

TABLE OF CONTENTS

LIST OF TABLES

TABLES

LIST OF FIGURES

FIGURES

CHAPTER 1

INTRODUCTION

1.1 Bending Process

Thin-walled beam bending processes have been adopted widely in the aerospace and automobile industries for their supplying much lighter products with adequate strength. Bending has some advantages in comparison with conventional manufacturing processes such as welding. It can reduce the weight of the component and reduce tooling cost due to fewer parts [1].

Beam bending applications range from simple household items to complex industrial parts such as vehicle chassis. In beam bending processes, both open and closed sections can be bent into desired radius. One of the most commonly used closed section beam type is tube, and wherever tubes are used, the accurate bend angle and proper cross section are usually desired.

In tube bending processes, the commonly faced problem is cross section distortion of tube in the bent region. Tube hydroforming has been identified as a new technology to give desired shapes to closed sections. In most cases, the first step of hydroforming is bending of the tube to a required shape. The tube is bent to the approximate centerline of the final part to enable the tube to be placed in the die cavity [2].

In both open and closed section beam bending operations, there is one thing that cannot be predicted before unloading, springback angle. Due to material elasticity, a bent profile springs back after unloading. In order to bend a profile to a desired angle, one must know that the springback beforehand. Then the profile is overbent so that the unloaded profile angle equals the desired angle. Unfortunately, the springback angle depends on many factors such as bend angle, profile material, profile dimensions, bend radius and so on. The traditional trial-and-error method has some problems of high scrap rate, low efficiency and operator experiences dependency [3].

1.2 Types of Bending Processes

Cold bending of metal profile products is probably one of the oldest metal forming processes and the bent parts are widely used in the industry. There are several methods to be used for cold bending production such as rotary draw bending, compression bending, roll bending and stretch bending. The most popular methods are the rotary draw bending and compression bending because of less setup time, less tooling cost and no lubricant needed. Both of them can be embodied in either manual benders or powered bending machines [4].

1.2.1 Rotary Draw Bending

Rotary draw bending is the most commonly used bending method and is used widely in many industries due to its low tooling cost. The tooling mainly consists of a bend die, clamp die, pressure die and wiper die (Figure 1.1).

In this method, the workpiece is clamped to a rotating form and drawn by the form against a pressure die. The pressure die can be either fixed or movable along its longitudinal axis. A fixed pressure die must be able to withstand abrasion caused by the sliding of the work metal over its surface. A movable pressure die, because it moves forward with the workpiece as it is bent, is less subjected to such abrasion. It provides better guidance and more uniform restraint of the work material [5]. For closed sections, a mandrel along with wiper die is sometimes used to prevent the collapse of the profile. However, the use of mandrel should be avoided if possible, since it increases the production cost [6].

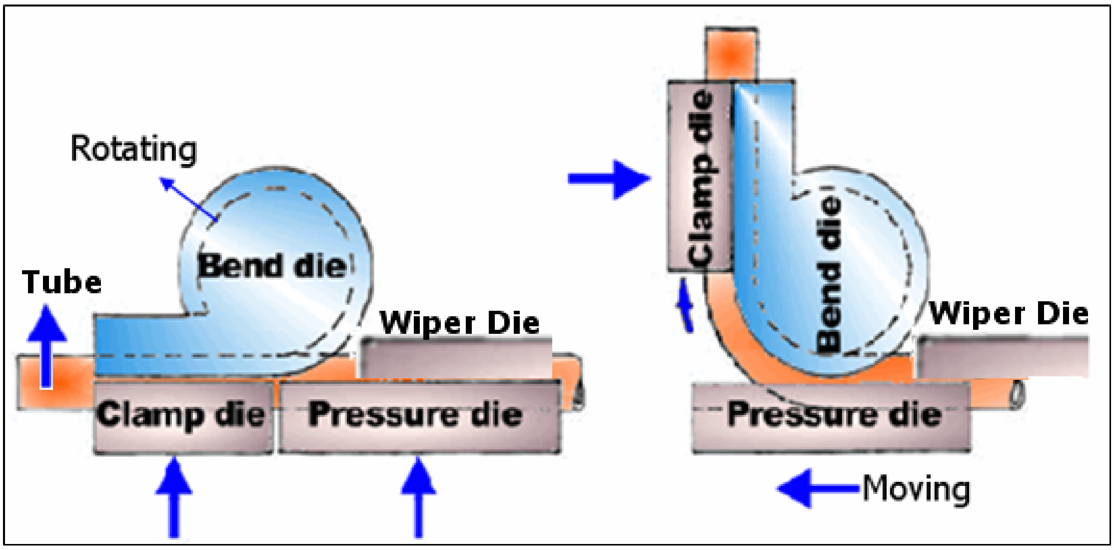

Figure 1.1 Rotary Draw Bending Tooling [7].

1.2.2 Compression Bending

The tooling for the compression bending is similar to rotary draw bending. The tooling mainly consists of bend die, clamp die and wiper die. The only difference between rotary draw bending and compression bending is that in rotary draw bending the bend die is rotating with clamp die, whereas in compression bending the bend die is stationary and wiper die is rotating around the bend die. In this method, the workpiece is clamped to a fixed form, and a wiper shoe revolves around the form to bend the workpiece [5]. Figures 1.2 shows initial and final configurations of compression bending.

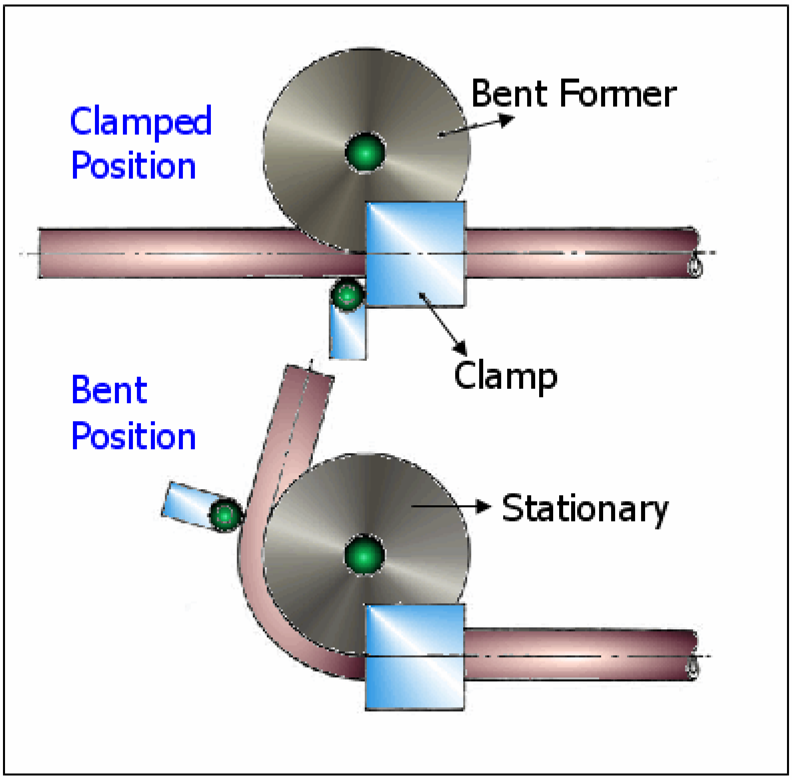

Figure 1.2 Initial and Final Configurations of Compression Bending [7].

1.2.3 Roll Bending

In roll bending operations, three or more parallel rolls are used. In one arrangement using three rolls, the axes of the two bottom rolls are fixed in a horizontal plane. The top roll (bending roll) is lowered toward the plane of the bottom rolls to make the bend (Figure 1.3). The three rolls are power driven; the top roll is moved up or down by a hydraulic cylinder [5].

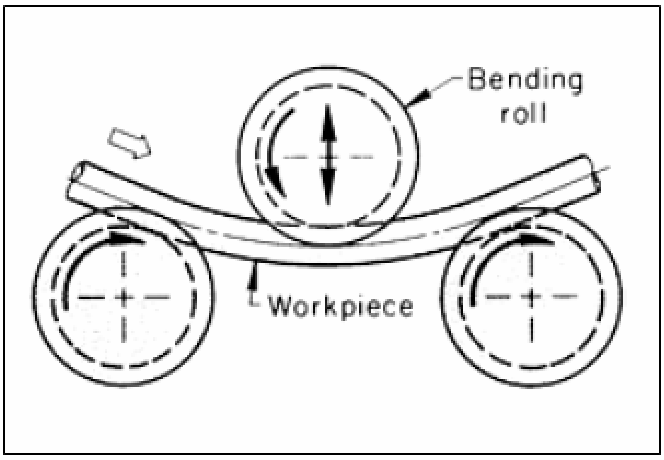

Figure 1.3 Operating Essentials of Three Roll Bending [5].

Roll bending is impractical for making more than one bend in a bar. It is difficult to control springback in a roll bender, and it may take several passes through the rolls to make the needed bend. Therefore, this method of making bends is slower than other methods [5].

1.2.4 Stretch Bending

In this method, the workpiece is first gripped by jaws which are mounted on hydraulic actuators. The workpiece is then stretched axially to a chosen value of tension, and then the bending die moves upward while the tension is kept constant (Figure 1.4) [8]. Usually, less springback occurs when the work is bent while it is stretched [5].

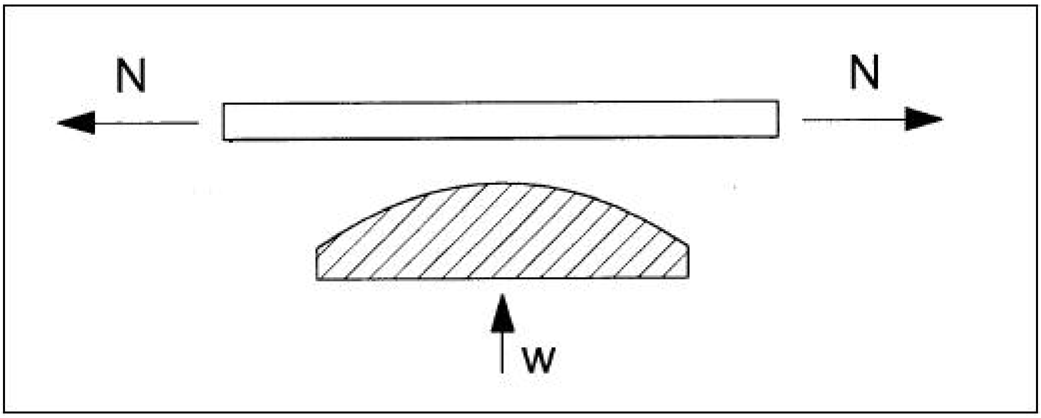

Figure 1.4 Stretch Bending Process [9].

1.3 Defects in Bending Processes

During bending process, the workpiece undergoes several defects such as springback, cross-section distortion, wrinkling and fracture.

1.3.1 Springback

After bending operations, springback is inevitable phenomenon when the load is released due to the elastic property of the material. This leads to an increase in the radius of curvature and a reduction in the bending angle of the bent workpiece. Further leads to the decrease of the dimensional accuracy of the workpiece and makes it difficult to fit with others [10].

During bending process, there exist stresses in the workpiece. While the outer side of the workpiece (extrados) is subjected to tensile stress, the inner side of the workpiece (intrados) is subjected to compressive stress. Because of these opposite stresses, the workpiece springs back in a rotating manner (Figure 1.5).

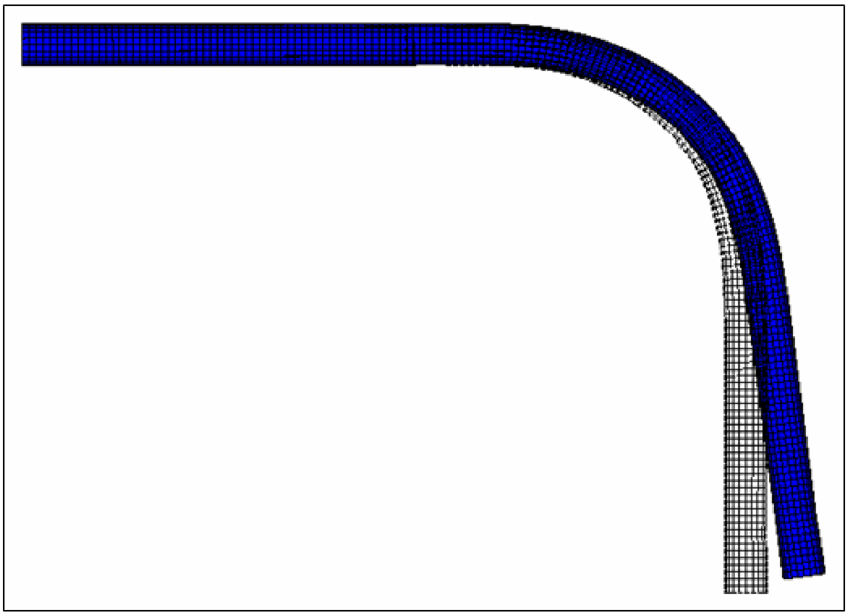

Figure 1.5 Springback of a Bent Tube.

1.3.2 Cross-Section Distortion

For closed sections like tube, the common cross-section problems are wall thickness change and flattening. Since the outer side of the tube is subjected to tensile stress, its thickness at the outer side decreases. And since the inner side of the tube is subjected to compressive stress, its thickness at the inner side increases (Figure 1.6). The flattening results from collapsing outer surface of tube, since there is no internal resistance to the tube (Figure 1.7).

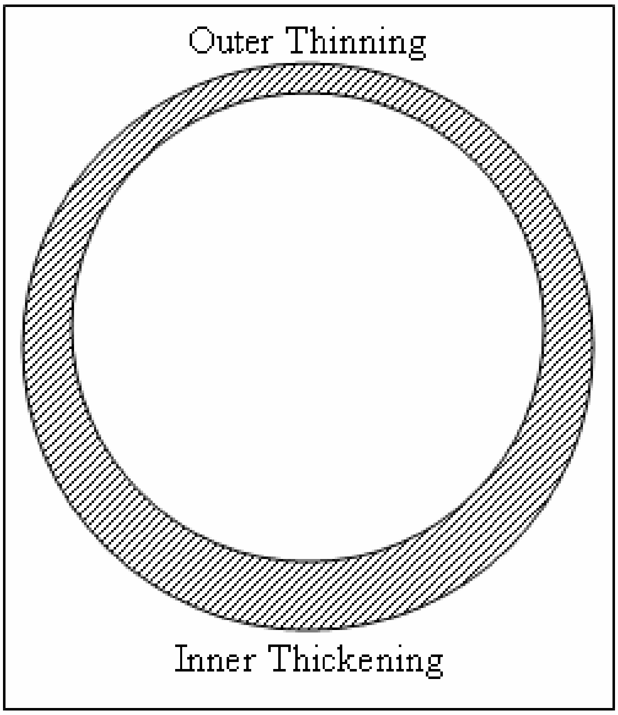

Figure 1.6 Wall Thickness Change in a Bent Tube.

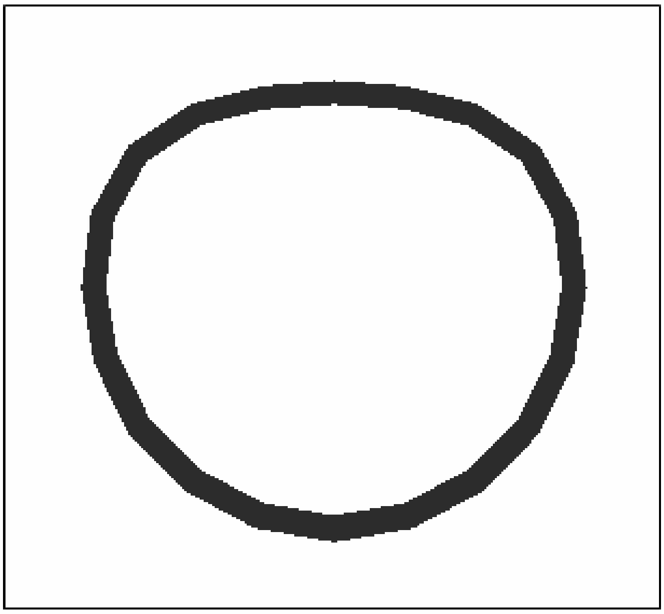

Figure 1.7 Flattening in a Bent Tube.

1.3.3 Wrinkling

When a thin walled beam is bent, there exist compressive stresses in the inner side of the workpiece. If this compressive stresses are high, the inner surface of workpiece buckles and wrinkling occurs (Figure 1.8). This wrinkling phenomenon occurs, if the process parameters are inappropriate especially for tubes with large diameter, thin wall thickness and tight bend radius [11].

Figure 1.8 Wrinkling in a Bent Tube [11].

1.3.4 Fracture

The outer surface of thin walled beams is subjected to tensile stress during bending operations. When the stress generated in the outer surface exceeds ultimate tensile strength value, the material starts necking and then fails.

1.4 Advantages of Additional Loading

Two types of additional loadings can be applied during bending process. One loading type is a boundary constraint which is fixing one end of tube during bending process. The other additional loading type is internal pressure.

1.4.1 Fixing One End

The main purpose of fixing one end is to reduce the compressive stress at the intrados.
When a workpiece is bent, tensile stress is shown at the extrados and compressive stress is shown at the intrados. If the workpiece is fixed from one end, this compressive stress values are reduced by this stretching effect. Therefore, the springback angles are also reduced.

1.4.2 Internal Pressure

The aim of using internal pressure is to overcome cross-section distortion of tubes. In rotary draw tube bending processes, since there is no internal resistance to the surface, the tube surface at the extrados loses its ovality and this is called flattening. If internal pressure is used during bending process, the pressure provides an internal resistance to the tube and flattening can be avoided. Furthermore, in bending operations the thickness of beam at intrados increases and the thickness of beam at extrados decreases. Internal pressure also decreases this thickening at the intrados. Beside this, the internal pressure increase wall thinning at the extrados.

There is another method called hydroforming giving the tube a proper cross-section. In hydroforming processes, the tube requires prebending as a performing operation. The tube must be bent to the approximate centerline of the finished part prior to hydroforming to enable the tube to be placed in the die cavity. The tube is then placed into the die and die closes. Hydraulic fluid fills the tube with two side cylinders closing around the ends of the tube. Simultaneously, the liquid is pressurized and cylinders are pushed in from side. The material of the tube yields and flows into the die cavity and the part is formed [6].

On the contrary, in push-bending process, in order to provide internal pressure, an incompressible elastic material is used. The principle of the method is that a male die pushes a tube into a bend female die to make it deform to the desired bend shape, whilst at the same time, an elastic material filling the tube is compressed by a spherical mandrel to generate internal pressure [15]. Figure 1.9 shows the tooling of push bending process described above.

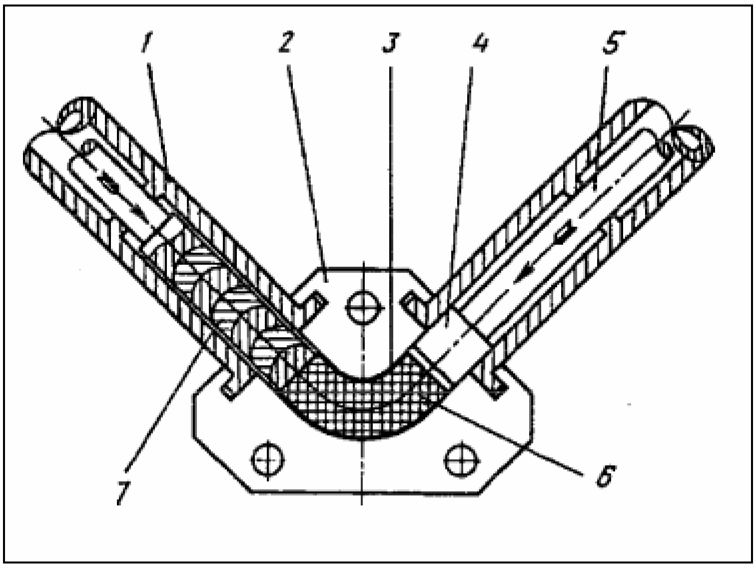

Figure 1.9 The push-bending principle in the forming of a small bend radius tube. (1) The guide sleeve, (2) the female die, (3) the part, (4) the male die, (5) the push mandrel, (6) the elastic material, (7) the spherical mandrel [15].

1.5 Aim and Scope

Springback and cross-section distortions are two severe defects in rotary draw bending operations. Industry practice for springback phenomenon is overbending of beam. However, the traditional trial-and-error method has some problems of high scrap rate, low efficiency and operator experiences dependency [3]. Moreover, in order to overcome cross-section distortion, tube hydroforming has been identified as a new technology to give desired shapes to closed sections [2]. However, this method needs additional tooling, since hydroforming is performed after bending process.

In this study, a detailed investigation of finite element analyses of forming of thin walled aluminum beams is performed using finite element simulations to model rotary draw bending processes.

In third chapter, the main idea is to investigate the springback behavior of different beam types for various bend radius and wall thickness. In the analyses, three types of beams are used which are T-Shaped, U-Shaped and tubular. For T and U-Shaped beams, the bend radiuses of 100, 110, 120,130 mm and thicknesses of 1, 2 and 3 mm are used. For tubular beam, the bend radiuses of 70, 80, 90, 100 mm and thicknesses of 1, 2 and 3 mm are used. Afterwards, experiments for a tube having 20 mm diameter, 100 mm bend radius and 1 mm wall thickness are performed and experimental results are compared with simulation results. Moreover, for a chosen tube dimension and bend radius, the springback behavior of this chosen tube is examined for different bend angles starting from 10^0 to 90^0. After a number of analyses, the effect of bend angles on springback is found in order to use that relation in overbending calculations. Furthermore, the study focuses on what if scenario. In all applications of rotary draw bending, the back end of workpiece is released so that the back end of workpiece moves together with the dies. In this case, for a chosen tube dimension and bend radius, springback comparison is examined between the same workpieces. Only the difference between these two workpieces is that one is free and one is fixed from the back. Moreover, the study deals with cross-section distortion problem in rotary draw tube bending processes. In this chapter, in order to overcome cross-section distortion problem, internal pressure is applied during bending operation. Therefore, the effects of internal pressure on cross-section and wall thickness are examined.

CHAPTER 2

LITERATURE SURVEY

2.1 Introduction

In this chapter, previous researches on bending operations are going to be summarized. The researches have been mainly focused on cross-section distortion and wall thickness change in pure bending operations. In 1927, Brazier [12] studied distortion of thin cylindrical shells. According to the results, the author analytically showed that the cross section of thin walled tube gained some ovality in pure bending operation.

Following the first basic researches, the studies gain acceleration with the expanding technology and changing forming operations. The studies can be classified according to the problems faced in bending of thin walled structures as follows.

- Studies on springback in bending processes,
- Studies on cross-section distortion in bending processes,
- Studies on hydroforming in bending processes,

2.2 Springback

Stelson and Lou [3] focused on springback behavior of thin walled tube after rotary draw bending process (Figure 2.1).

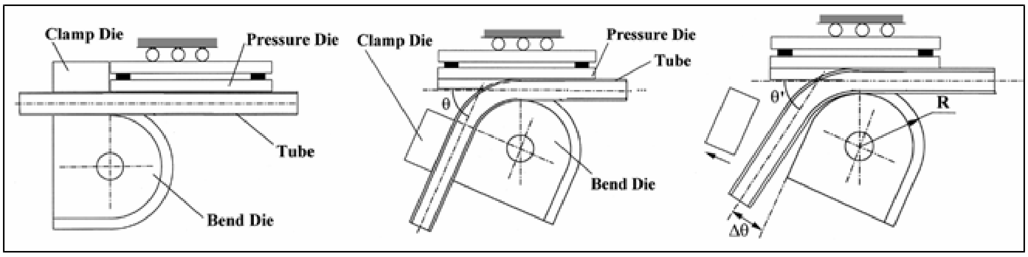

Figure 2.1 Rotary Draw Bending Process and Springback after Unloading [3].

The authors compared the springback results between one bend cycle to desired bend angle and rebend to desired bend angle with multiple cycles. All their experiments are performed with the same dimension tube and bend radius. Firstly, they examined the springback behavior of a tube for various bend angles. They found that for large bend angles (above 10^0) the springback behavior of that specific tube has a linear relationship with bend angles (Figure 2.2).

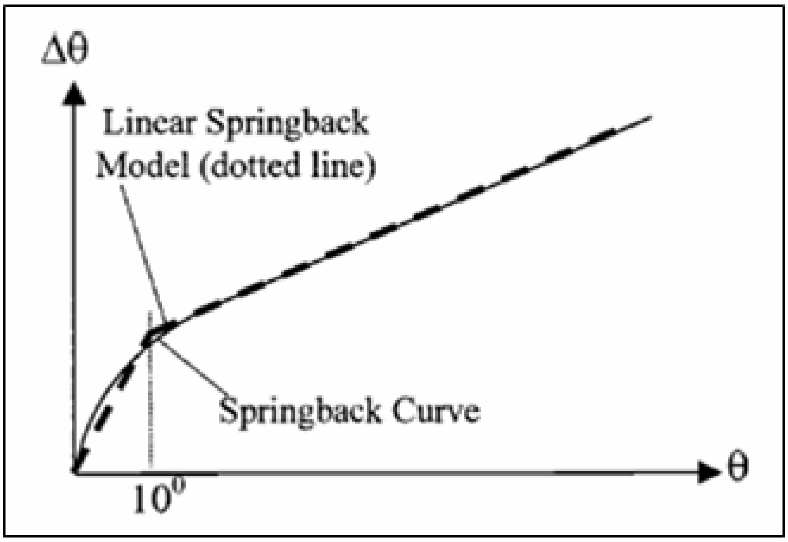

Figure 2.2 Springback Angle Δθ vs Loaded Bend Angle θ [3].

After this research, they focused on effects of additional loading cycle on springback, and concluded that the springback of a bend made by several loading cycles differs from the springback of the same bend if it were made by one loading cycle.

According to their research, it can be realized that when the additional rebend angle is larger, the reload effect becomes smaller. In general, the springback of a tube bent made by several loading cycles is smaller than the springback of the same tube if it were bent with one loading to the same target angle.

In recent years, analytical method and finite element method (FEM) are two main methods used to analyze the whole springback of tube bending processes [10]. Zhan, Yang, Huang and Gu [10] decided to examine the effects of material parameters in finite element analysis on springback angles. They used parametric material models in their finite element analysis. This particular study based on a specific tube dimensions which are outer diameter of 28 mm and thickness of 1 mm. The flow stress model used in the analyses is $\sigma = K\varepsilon^n$.

The changing parameters in the formulation are strength factor (K) and hardening exponent (n). Their starting point comes from stainless steel (1Cr18Ni9Ti) having strength factor of 1356 MPa and hardening exponent of 0.549.

After a series of analyses, they found that the larger the strength factor, the larger springback angle they had. The results for various strength factors are given in Figure 2.3.

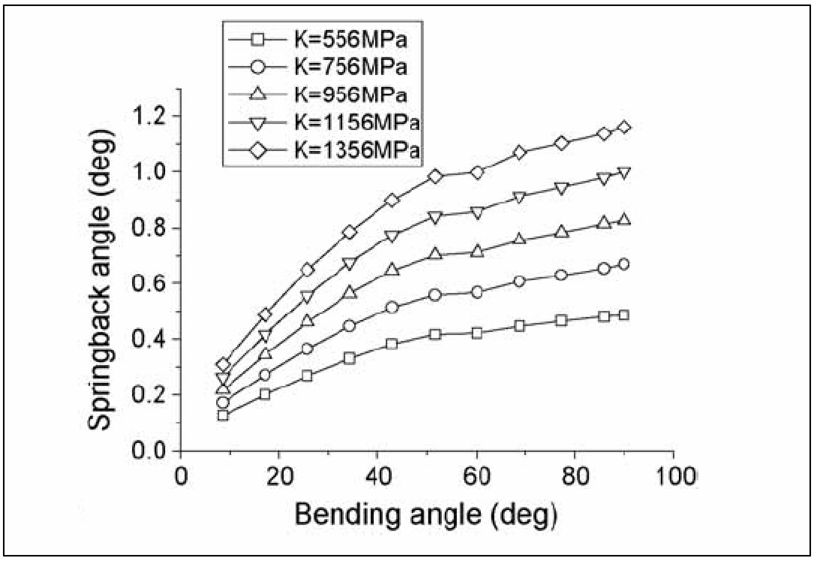

Figure 2.3 Effects of Strength Factor on Springback Angle [10]

Whereas, the larger hardening exponent, the smaller springback angle they had in their series of analyses. The results for various hardening exponents are given in Figure 2.4.

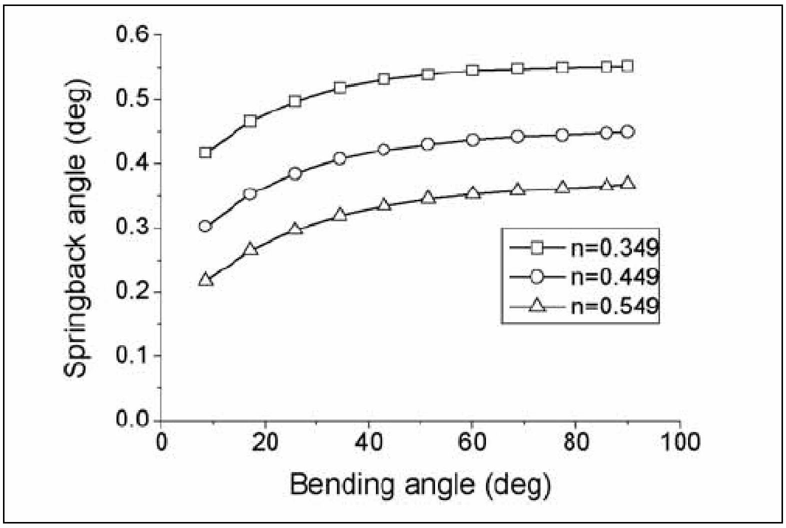

Figure 2.4 Effects of Hardening Exponent on Springback Angle [10]

2.3 Cross-Section Distortion

According to the studies and experiments performed so far, it is found that in tube bending processes the thickness of the tube changes over the circumference. The outer surface thickness of the tube decreases, whereas the inner surface thickness increases.

Tang [13] has improved an analytical method to predict wall thickness change in tube bending processes. The author's starting point for wall thickness prediction equation is deformation theory of plastic flow. He expressed strain and stress equations as follows.

$$\varepsilon_x = \frac{1}{E}\left[\sigma_x - \nu(\sigma_c + \sigma_r)\right]$$

$$\varepsilon_c = \frac{1}{E}\left[\sigma_c - \nu(\sigma_r + \sigma_x)\right]$$

$$\varepsilon_r = \frac{1}{E}\left[\sigma_r - \nu(\sigma_x + \sigma_c)\right] , \tag{1}$$

where $\varepsilon = \Delta l / l$ is the deformation of unit length, E is the elastic modulus of tube material and ν is Poisson ratio. And his assumption is that since wall thickness is smaller compared to the tube radius, the radial stress σ_r is negligible. After a series of substitutions, the author found the following equation for outer thinning.

$$t_o = \left(1 - \frac{2k + \cos\alpha}{4k + 3 - \cos\alpha}\frac{\cos\alpha}{2k}\right)t , \tag{2}$$

And the following equation for inner thickening.

$$t_i = \left(1 - \frac{2k + 2 - \cos\alpha}{4k + 1 + \cos\alpha}\frac{\cos\alpha}{2k}\right)t , \tag{3}$$

In his equations, there is an important variable which is α that defines the location in the cross-section to find the wall thinning and thickening. α is defined between $0^0 - 90^0$ for thinning equation, and α is defined between $90^0 - 180^0$ for thickening equation. The cross-section properties are shown in Figure 2.5.

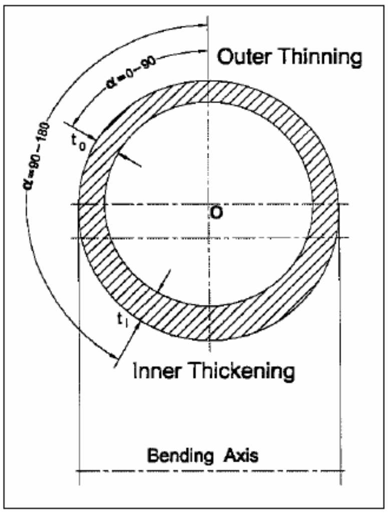

Figure 2.5 Cross-Section Properties [13]

The author determined that "t" is the original wall thickness (undeformed tube thickness) and "$k = R/2r$". "R" is the bend radius and "r" is the radius of tube.

Since the maximum wall thinning occurs at the outermost point, by substituting α = 0 the minimum wall thickness can be found as follows.

$$t_{om} = \left(1 - \frac{2k+1}{2k(4k+2)}\right)t, \tag{4}$$

As in thinning equation, in this case the maximum thickening occurs at the innermost point, and by substituting $\alpha = 180^0$, the maximum wall thickness can be found as follows.

$$t_{om} = \left(1 + \frac{2k+3}{8k^2}\right)t, \qquad (5)$$

Zhan, Yang, Jiang, Zhao and Lin [1] have prepared a finite element model to see the wall thickness change in tube bending process. In their model, the material used is 304 Stainless steel, tube has 28 mm outer diameter, 228 mm length and 1 mm thickness and the bend radius is 56 mm. As expected, they found tensile stress at the outer surface of tube and compressive stress at the inner surface of tube (Figure 2.6).

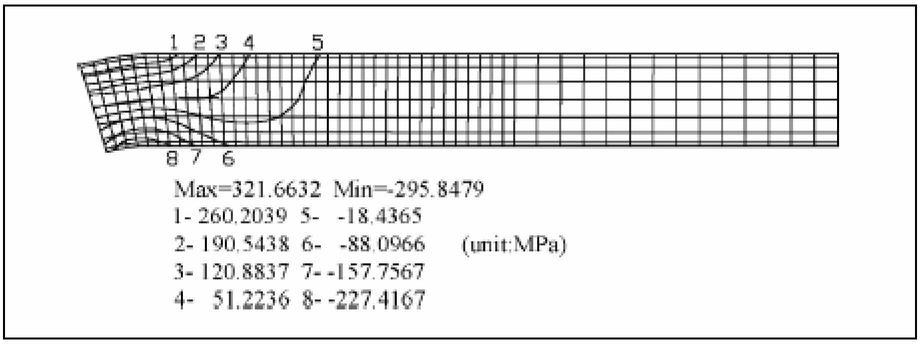

Figure 2.6 Stress Distribution Along the Bending Direction of Tube [1]

Their second observation is that the maximum wall thickness reduction ratio in the outer tensile area changes only a little with increase of bending angle, while the maximum wall thickness increase ratio in the inner compression area increases linearly with bending angle as shown in Figure 2.7.

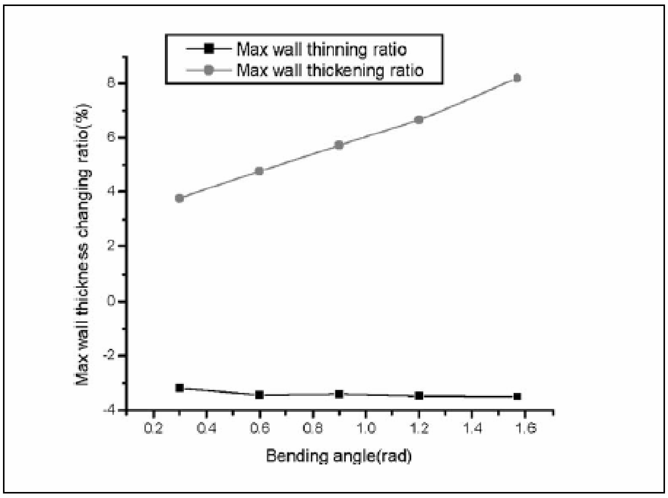

Figure 2.7 Relationship Between Thickness Changing Ratio and Bend Angle [1]

Lee, Van Tyne and Field [14] showed that in the manufacturing of some parts, pre-forming operations are often required prior to tubular hydroforming process. During some pre-forming processes, the cross-section of a bent circular tube goes into an oval-like shape and sometimes hoop-buckles. Therefore, they decided to use oval tube in order to eliminate this hoop-buckling phenomenon. In their research, they present detailed parametric studies on the bending of oval tubes. The finite element modeling technique is used to examine the deformation characteristics such as flattening and hoop-buckling for both circular and oval tubes.

They started their research with bending of two different cross-section beams which are circular ($\gamma = 1$) and oval shape ($\gamma = 0.5$). γ shows the length ratio of long and short sides in cross section of beam (Figure 2.8). For this case, the bend radius is 175 mm, and wall thickness of beam is 2 mm.

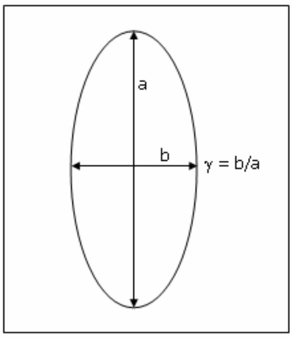

Figure 2.8 Definition of Ovality.

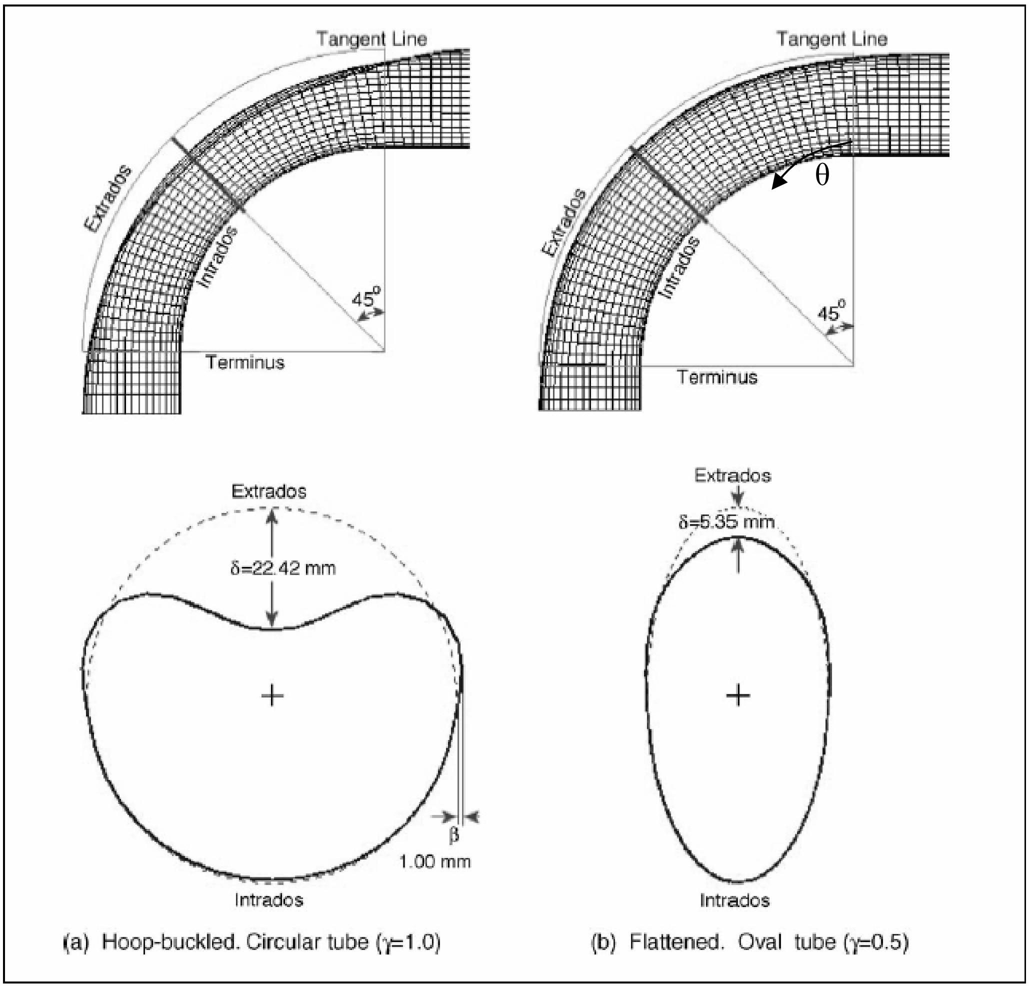

Figure 2.9 Cross Section Distortions of (a) Circular Tube and (b) Oval Tube [14]

When an oval tube with γ = 0.5 is bent under the same bending conditions as the circular tube shown in Figure 2.9 (a), the outside of the tube is not hoop-buckled, just flattened with a small amount of δ = 5.35 mm.

Then they extended this study in order to see the effect of bend radius on hoop-buckling phenomenon for an oval tube having γ = 0.5. They also found that the maximum hoop-buckling occurred at almost 35^0 angles on the tangent line shown in Figure 2.10.

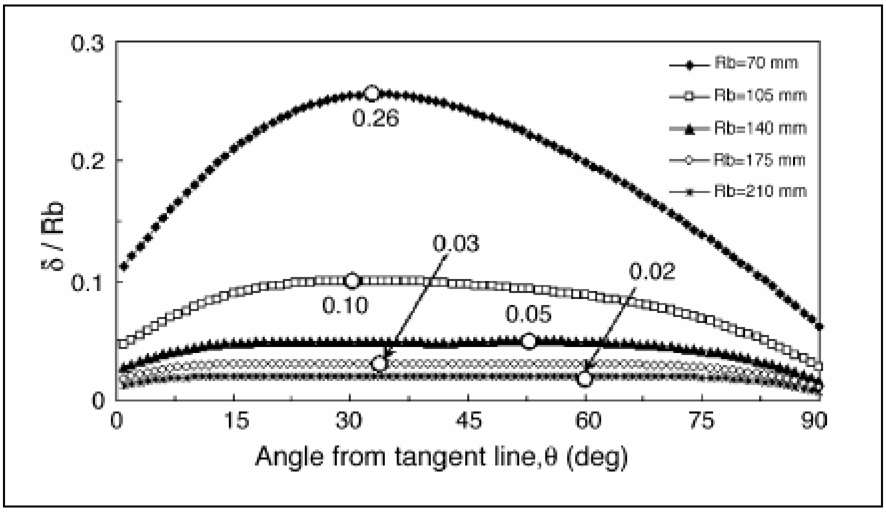

Figure 2.10 Non-dimensional δ/R_b as a Function of Angular Position Along the Bend (θ) Measured From the Tangent Line for $\theta_b=90^0$, γ=0.5 and t=2 mm. (δ:extrados flattening, R_b: Bend Radius) [14]

As it can be seen from Figure 2.10 that when bend radius is increased the maximum value of δ/R_b ratio decreases, and also maximum value of δ decreases. The second trend that can be extracted from Figure 2.10 is that when bend radius is increased the flattening (δ) along the bend tends to be constant.

Their final study in this research is to see effects of wall thickness and ovality (γ) on maximum flattening and hoop-buckling. The maximum flattening distance measured along the outside of the bend is defined as δ_{max} regardless of whether hoop-buckling occurs or not. Figure 2.11 presents the maximum amount of flattening (δ_{max}) predicted in tubes with constant bend radius (R_b = 175 mm). A line divides the hoop-buckled region from the region with only flattening. All of the circular tubes hoop-buckled because the unsupported bend of the circular tube did not have sufficient stiffness. However, most of the oval tubes are flattened without hoop-buckling except for oval tube having γ = 0.8 and thickness of 1.5 mm.

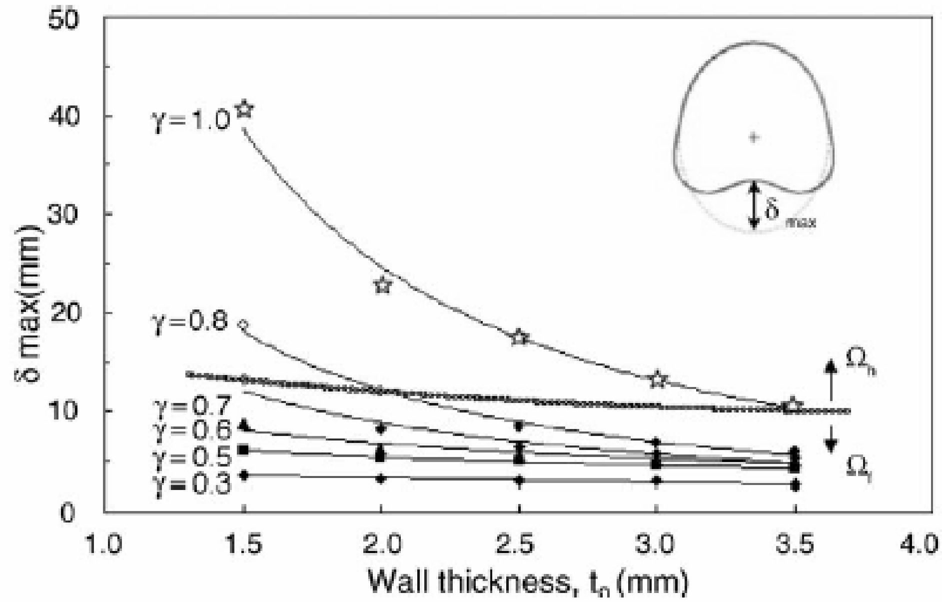

Figure 2.11 Maximum amount of flattening (δmax) as a function of the wall thickness with *R*b = 175 mm. (*Ω*f: flattened region without hoop-buckle,*Ω*h: hoop-buckled region) [14]

2.4 Hydroforming

Yang, Jeon and Oh [6] simulated prebending and hydroforming processes that are used to form an automotive part. The first step of the operation is prebending. In prebending step, the springback effects are taken into account so that the bend angles are increased (tube is overbent) and this recovery situation is tolerated with overbending of tube. After a number of bending operations, the rough shape of the tie bar is obtained. The second step of the operation is hydroforming. In this hydroforming step, the finite element model is composed of the prebent tube, a lower die, and an upper die. When lower and upper dies are closed, the existing shape between the dies is exactly the shape of tie bar as desired. In the analysis, the maximum internal pressure used is 60 MPa. Figure 2.12 shows the finite element model prepared for hydroforming process.

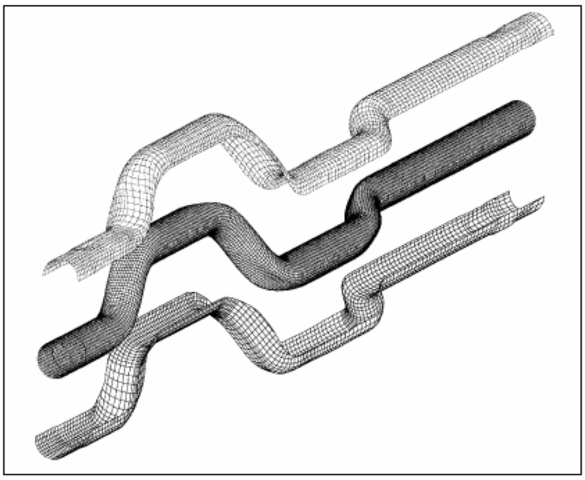

Figure 2.12 Prebent Tube and Hydroforming Dies [6]

When hydroforming simulations are finished, they obtain the final shape of tie bar as shown in Figure 2.13.

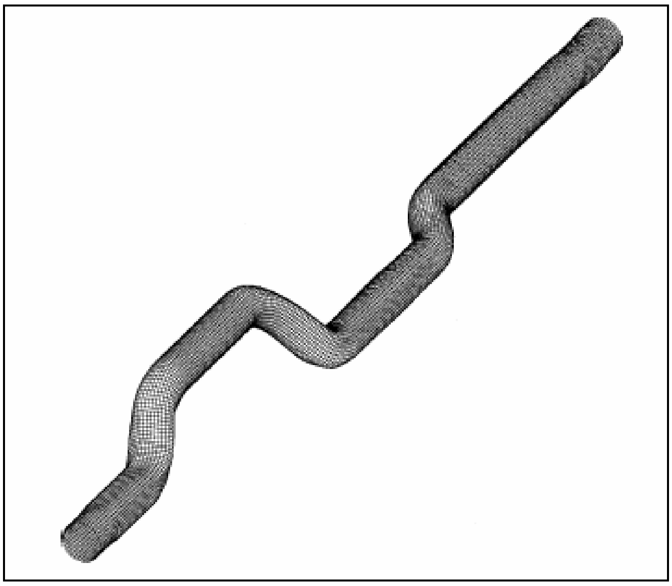

Figure 2.13 Predicted Final Geometry of the Tie Bar [6]

After prebending simulations, by applying 60 MPa internal pressure, they performed hydroforming simulations. And according to their results, the tie bar got its final shape without any defects. The only defect that they faced is extreme wall thinning. In some bent regions the wall thickness decreases to 1.4 mm from 2 mm.

Zeng and Li used tubular aluminum alloy workpiece subjected to 5MPa and 50 MPa internal pressures in their push-bending experiments. In order to apply different the internal pressure values, they changed the mandrel force according to the formula $P_R = pA$, where "p " is internal pressure required, "A" is cross-sectional area of the bore of the tube and "P_R" is the mandrel force applied.

According to their experimental research, they concluded that when the internal pressure applied is 5 MPa, there exist many wrinkles on the bent tube. Whereas, when the internal pressure is increased up to 50 MPa, the tube is bent perfectly and the wrinkling phenomenon is overcome. The experimental results for effects of internal pressure on bending performed by Zeng and Li can be seen in Figure 2.20.

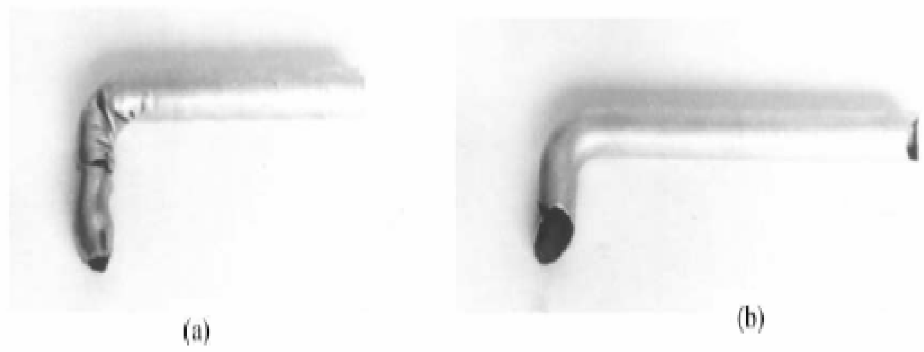

Figure 2.14 Experimental Parts of Aluminum Alloy Formed Under Different Pressures: (a) p = 5 MPa and (b) p = 50 MPa [15]

Gao and Strano [16] investigated the effect of pre-bent tube radius on hydroforming process. Their plan is to make possible modification on bending radius in rotary draw bending process prior to hydroforming process which has a specified hydroforming tooling, in order to form a specified tube successfully. Their comment at the beginning of the study was that the larger bend radius they use, the less thinning they will face after rotary draw bending process.

After performing FEM simulations of hydroforming of a pre-bent tube with a greater bending radius, their experiences are verified. The thinning for hydroformed tube is decreased from 27.86 to 24.92% as shown in Figure 2.15.

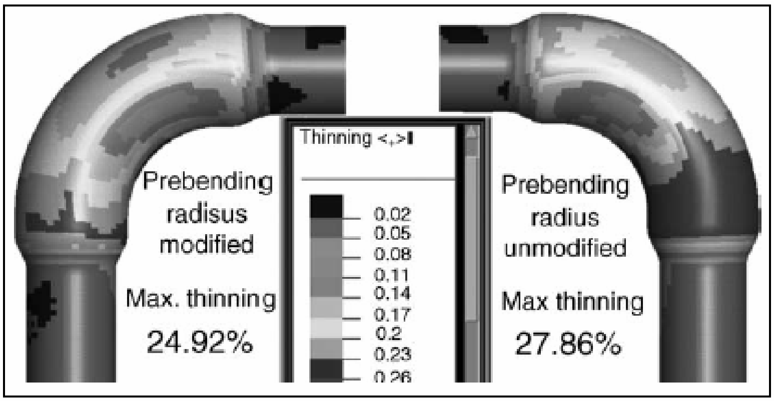

Figure 2.15 Effect of Pre-Bent Radius on Thinning of Final Part [16]

Wang and Agarwal [17] improved an analytical method, in order to predict the wall thickness change of a 90^0 bent tube in rotary draw bending process as Tang [13] did. However, there is an additional external load applied in their operations which is internal pressure.

They started their approach with basic principles based on plasticity theory. After a series of formulations, they found two equations that give the thickness values at extrados and intrados.

Finally, in order to validate their analytical method for wall thinning prediction, they prepared a finite element model, and they compared the results in two way. They first compared the wall thickness values with no internal pressure. Then they applied an internal pressure in the simulation, and compared results with analytical results. It can be seen from Figure 2.16 that the analytical results and finite element analysis results are in good agreement

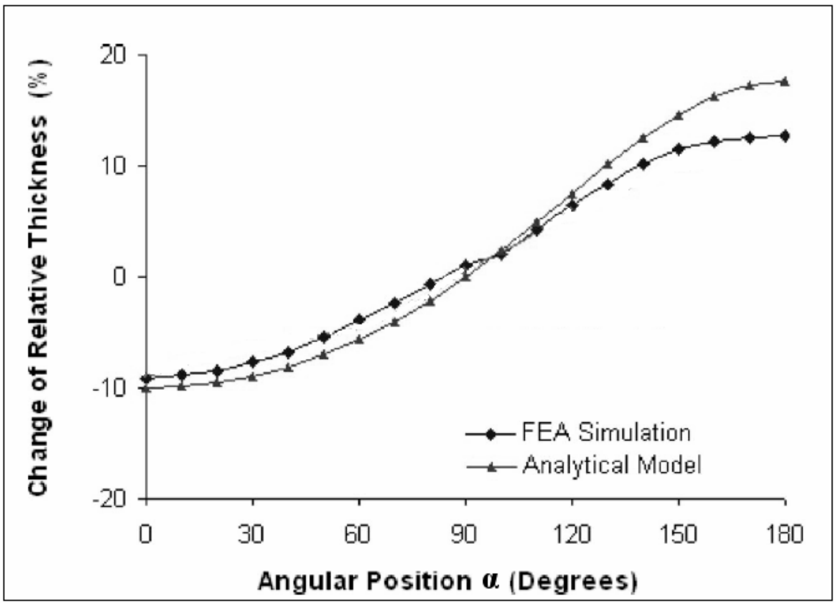

Figure 2.16 Comparison of Wall Thickness Prediction by Analytical and FEA Model [17]

After this validation, they applied an internal pressure of 10 MPa in analytical model and finite element model. Their results show that (Figure 2.17) when an internal pressure is applied to tube, the wall thinning at extrados increases, while wall thickening at intrados decreases. It can be said that wall thickening prediction by analytical model fits to finite element analysis results quite well. However, the results obtained for thinning by analytical method deviates from finite element analysis results much.

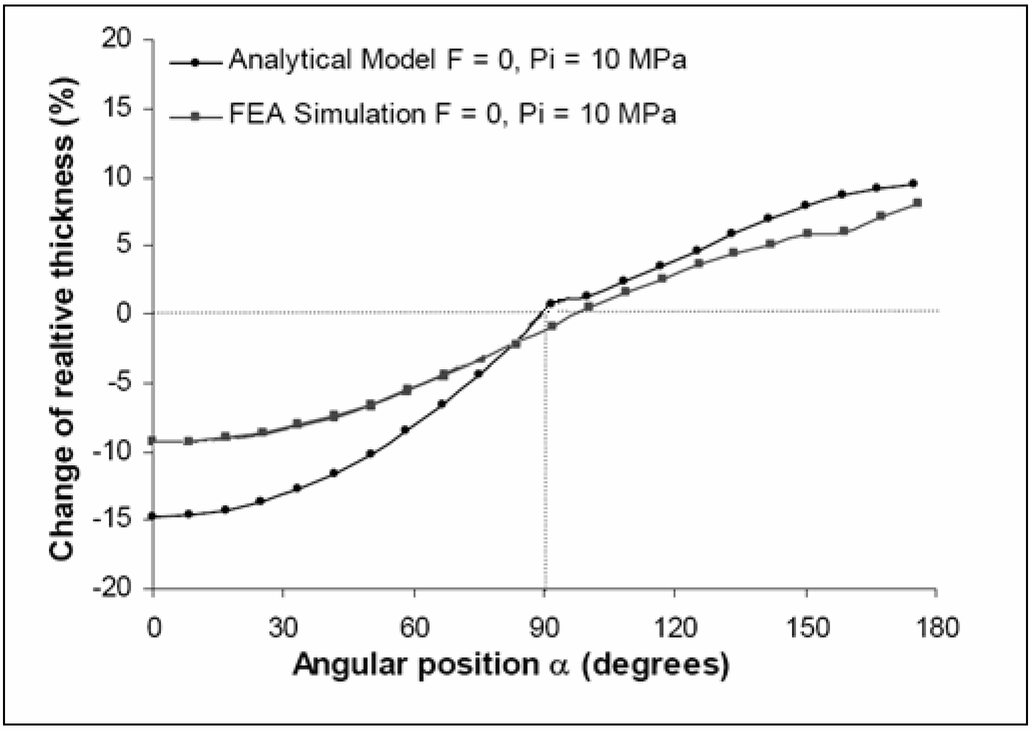

Figure 2.17 Comparison of Wall Thickness Prediction by Analytical Model (No Axial Pull, 10 MPa Internal Pressure) and FEA Model (No Axial Pull, 10 MPa Internal Pressure) [17].

CHAPTER 3

RESULTS

3.1 Bending Analyses of T-Shaped Beams With Respect To Various Bend Radius and Wall Thickness

T-shaped beam is one of commonly used beam types in the market. In this section, rotary draw bending operation is used to simulate bending operation of the beams. The aim of the analyses is to investigate the wall thickness change after bending operations and springback behavior after unloading conditions. While performing finite element analyses, the effects of bend radius and wall thickness values are considered.

The finite element models are prepared in commercial software ANSYS 11.0 for preprocessing. The analyses are solved by explicit software LS-Dyna, both ANSYS and LSPREPOST commercial codes are used for postprocessing.

3.1.1 Finite Element Analysis

For T-Shaped beam bending simulations, 12 different analyses are performed.

- Bend radius, R=100 mm for thickness, t = 1 mm, t = 2 mm and t = 3 mm.
- Bend radius, R=110 mm for thickness, t = 1 mm, t = 2 mm and t = 3 mm.
- Bend radius, R=120 mm for thickness, t = 1 mm, t = 2 mm and t = 3 mm.
- Bend radius, R=130 mm for thickness, t = 1 mm, t = 2 mm and t = 3 mm.

However, only the analyses results obtained for bend radius (R) of 100 mm and wall thickness of 1, 2 and 3 mm will be shown in details.

The dimensions of the beams are taken from standard manufacturing catalogues. Different bend radius values are used starting from 100 mm to 130 mm with 10 mm increments. The wall thicknesses are 1 mm, 2 mm and 3 mm for all those bend radiuses. The comparison between 1 mm, 2 mm and 3 mm thick beams is performed with respect to changing bend radiuses. The cross section specifications of the beams are shown in Figure 3.1. For all T-Shaped beams used in the analyses, a = 20 mm, b = 20 mm, however, s = 1 mm for thickness of 1 mm, s = 2 mm for thickness of 2 mm and s = 3 mm for thickness of 3 mm.

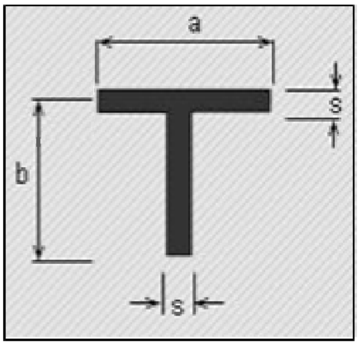

Figure 3.1 Cross-Section Details of T-Shaped Beams

Since the thickness value of the beam is much less than the cross-sectional and longitudinal dimensions of the beam, this structure is called thin-walled [18]. Therefore, shell elements are used (Shell163 in LS-DYNA), while preparing finite element model (Figure 3.2). Since die materials are considered as rigid compared with workpiece, the dies are defined as rigid in the analyses, i.e. non-deformable. The codes for preparing finite element model in ANSYS for a specific T-Shaped beam are given in Appendix A.

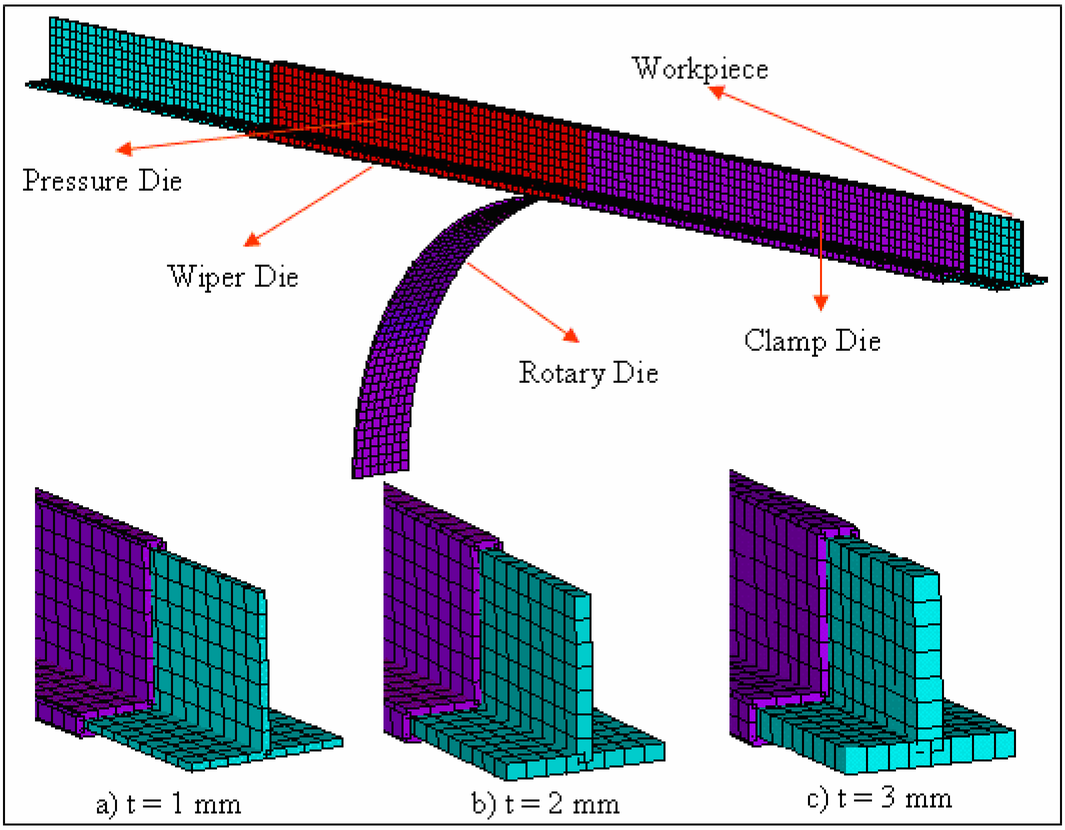

Figure 3.2 Finite Element Model for R=100 mm and a) t = 1 mm, b) t = 2 mm, c) t = 3 mm

Ls-Dyna theoretical manual says that for forming of thin walled aluminum workpieces, 3-Parameter-Barlat material model is suitable. The material chosen for the workpiece is Aluminum 6010. Therefore, 3-Parameter-Barlat material model constants are used for Aluminum 6010 in the analyses as shown in below.

Material Density	:	2,700 kg/m^3
Modulus of Elasticity	:	69,000 MPa
Poisson's Ratio	:	0.33
Strength Coefficient	:	503.9 MPa
Hardening Coefficient	:	0.245

3.1.2 Strains in Beams after Bending Operation

It has been experienced from previous studies that under the same conditions, maximum strain is observed in the beam which is bent to the smallest radius. Therefore, if the beam bent to 100 mm bend radius does not fail, the other beams bent to R = 110, 120 and 130 mm do not fail at all. The equivalent strain distribution for the beam which is bent to 100 mm radius is given in Figure 3.3.

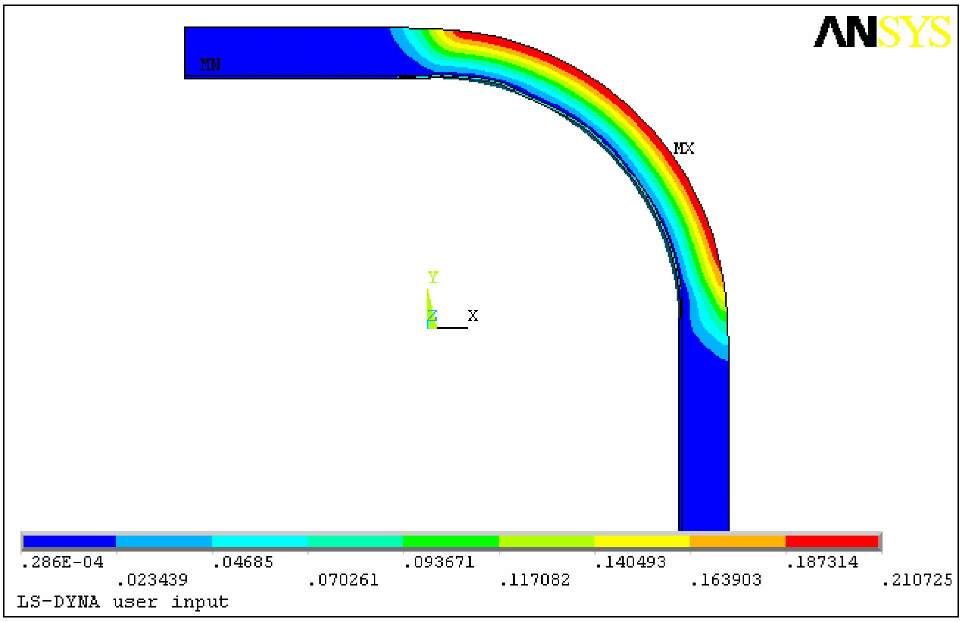

Figure 3.3 Total Equivalent Strain Distribution in Bent T-Shaped Beam for R=100 mm and t = 1 mm

As it can be seen in Figure 3.3, the maximum total equivalent strain value in the beam is 0.21. When the bend radius increases, the total equivalent strain in the beam decreases. Figure 3.4 shows the strain values for bending of T-Shaped beams having thickness of 1 mm.

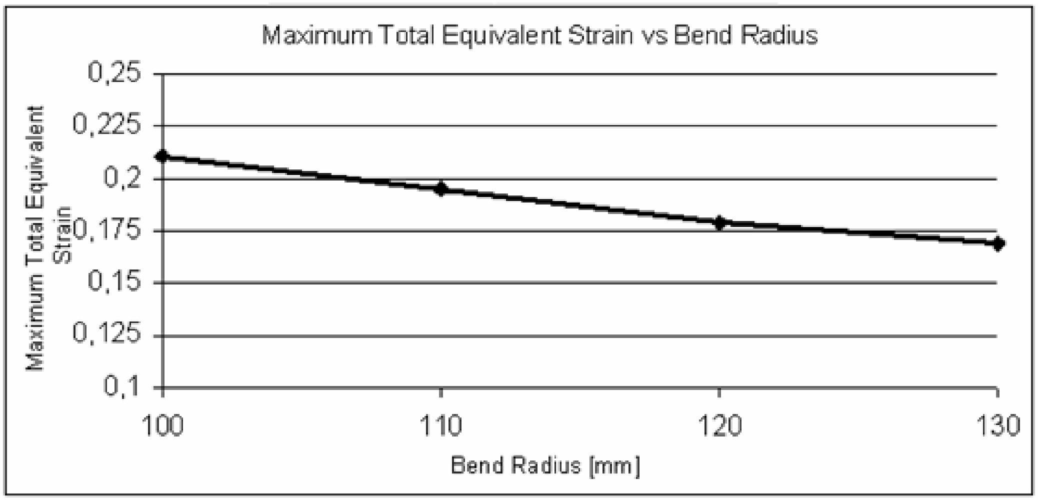

Figure 3.4 Max. Total Equiv. Strain Values wrt. Various Bend Radius for t =1 mm

3.1.3 Wall Thickness Change after Bending Operation

It is known that when a workpiece is bent to a radius, there exist tensile stress at the outer side and compressive stress at the inner side. Therefore, wall thinning is expected at the outer side and wall thickening is expected at the inner side. Figure 3.5 shows the wall thickness change in the beam having bend radius of 100 mm and wall thickness of 1 mm.

At the outer side, the minimum wall thickness is 0.91, and there exists wall thinning up to 8.9%. Since when the bend radius increases, the strain values decreases and the wall thinning in the bent beam also decreases. Figure 3.6 shows the wall thinning in terms of minimum wall thickness change with respect to bend radius for the beam having thickness of 1 mm.

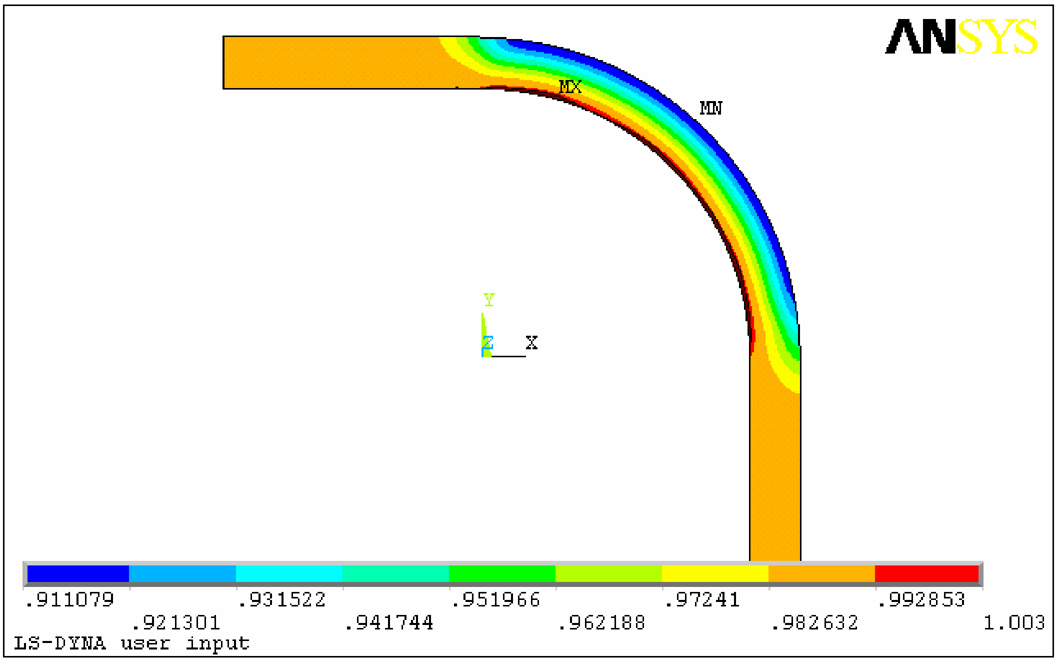

Figure 3.5 Wall Thickness Distribution in Bent T-Shaped Beam for R=100 mm and t=1 mm

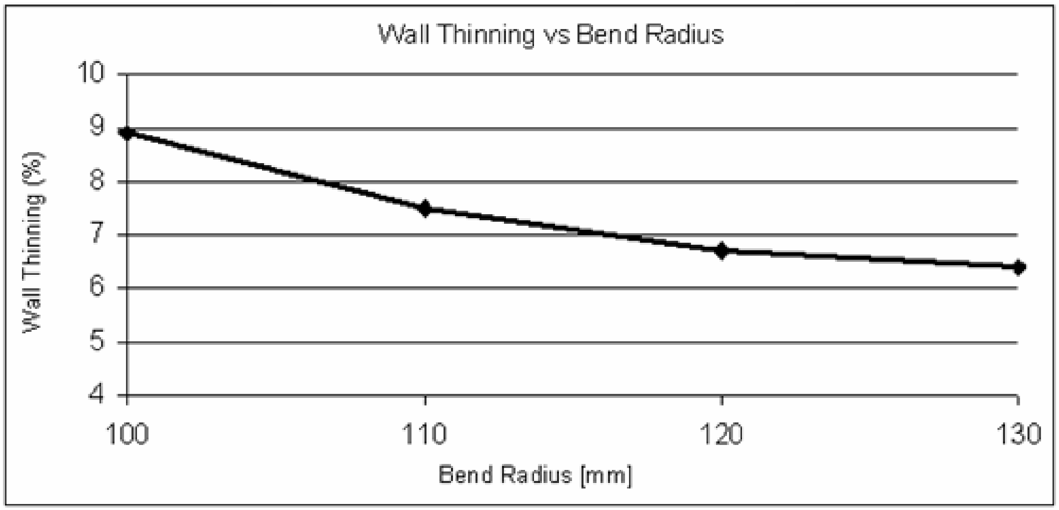

Figure 3.6 Wall Thinning With Respect To Various Bend Radius for t=1 mm

3.1.4 Springback Behavior after Unloading

In order to see springback behavior of T-Shaped beams after unloading, 12 different analyses are prepared. The models have bend radiuses of 100, 110, 120, 130 mm and wall thicknesses of 1, 2 and 3 mm. By this way, the effect of wall thickness and effect of bend radius on springback are investigated.

Bending analyses are performed in LS-DYNA software explicitly. Afterwards, the results taken from LS-DYNA are transferred to ANSYS to perform springback analyses implicitly (Figure 3.7).

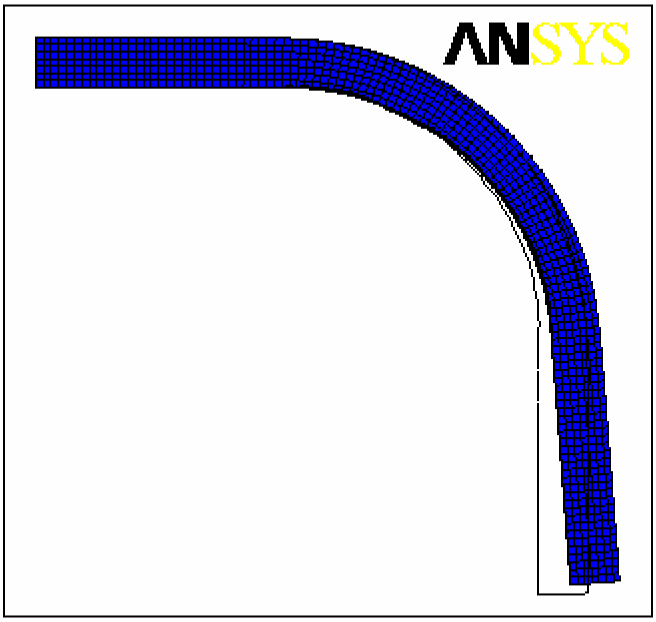

Figure 3.7 Springback after Unloading for R=100 mm and t=1 mm

It is observed that when bend radius increases, the total equivalent strain values decreases as it can be seen from Figure 3.4. Since the deformation is beyond elastic limit, the deformed beams undergo plastic deformations. Furthermore, it is known that the higher the plastic strain, the more strain hardening occurs. Therefore, the beams bent to small radiuses have higher strain values with higher strain hardening, and their mechanical strengths get higher. This phenomenon causes less springback after unloading. Therefore, the beams bent to smaller radiuses show less springback under the same conditions.

In bending operations of T-shaped beams, the springback behavior after unloading has a linear increasing tendency for various bend radiuses under the same conditions (Figure 3.8). The fitted lines to the scattered data give the formulas where θ in degree and R in mm,

$$\theta_{spring} = 0.017R_{bend} + 3.732 \qquad \text{for } t = 1 \text{ mm}$$

$$\theta_{spring} = 0.032R_{bend} + 3.466 \qquad \text{for } t = 2 \text{ mm}$$

$$\theta_{spring} = 0.038R_{bend} + 3.221 \qquad \text{for } t = 3 \text{ mm}$$

By using these formulas, the springback angle can be predicted beforehand. However, since the finite element model is prepared for this specific dimensioned model, the formulas can only be used for the particular material and dimensions selected.

It is seen that when wall thickness increases, the springback angles also increase. Therefore, if a beam having higher wall thickness is bent to a radius, the beam should be overbent more than a beam having wall thickness less for the same geometry.

It is observed that for all wall thickness values, the springback behavior has a linear tendency with respect to different bend radiuses. When the wall thickness is increased, the springback angles also increase. However, this increase has a decreasing tendency. The difference between $t = 1$ mm and $t = 2$ mm is higher than the difference between $t = 2$ mm and $t = 3$ mm.

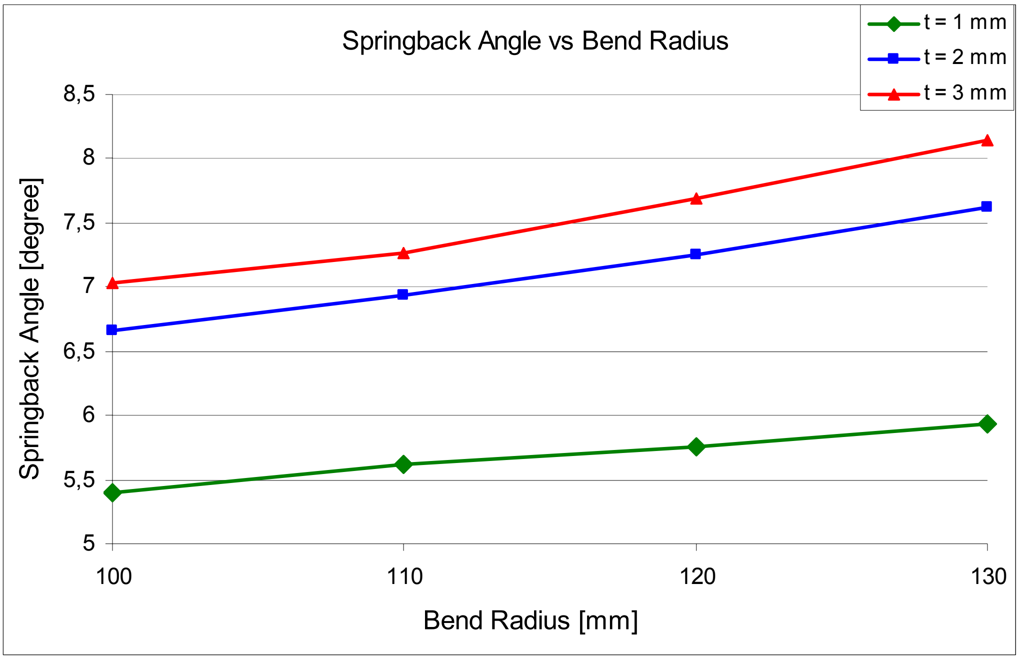

Figure 3.8 Springback Angle Comparison for Wall Thicknesses of 1, 2 and 3 mm

This result is in contradiction with sheet metal bending operation where thickness increases, springback decreases. The sample result of sheet metal bending simulation is given in Appendix B. In sheet metal bending, equivalent strain increases as thickness increases, and springback angles decreases. In this study, however, increasing thickness results in decreasing equivalent strain, and increasing springback.

3.2 Bending Analyses of U-Shaped Beams With Respect To Various Bend Radius and Wall Thickness

Rotary draw bending simulations of a commonly used beam type of U-shaped are performed in order to examine the wall thickness change behavior after bending and springback behavior after unloading. In the finite element analyses, bend radius and wall thickness values are varying parameters.

3.2.1 Finite Element Analysis

For U-shaped beam bending simulations, 12 different analyses are performed.

- Bend radius, R = 100 mm for thickness, t = 1 mm, t = 2 mm, t = 3 mm.
- Bend radius, R = 110 mm for thickness, t = 1 mm, t = 2 mm, t = 3 mm.
- Bend radius, R = 120 mm for thickness, t = 1 mm, t = 2 mm, t = 3 mm.
- Bend radius, R = 130 mm for thickness, t = 1 mm, t = 2 mm, t = 3 mm.

However, only the analyses results obtained for bend radius (R) of 100 mm and wall thickness of 1, 2 & 3 mm will be shown in details in this part.

The dimensions of the beams are taken from standard manufacturing catalogues. While performing finite element analyses, the changing parameters are chosen such that the bend radiuses varied from 100 mm to 130 mm with 10 mm increments and the wall thicknesses are 1 mm, 2 mm and 3 mm for all bend radiuses. Therefore, by combining these various parameters, 12 different analyses are performed. The dimensions of U-shaped beam are 40 mm width, (a), 20 mm height, (b), 1,2,3 mm thicknesses, (s). Figure 3.9 shows the cross-sectional details of chosen U-Shaped beams.

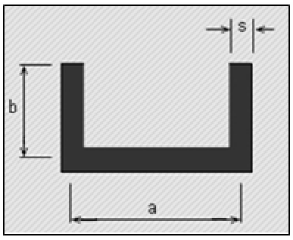

Figure 3.9 Cross-Section Details of U-Shaped Beams.

Figure 3.10 shows the finite element model used for bend radius of 100 mm, wall thicknesses of 1, 2 and 3 mm. Since the model confirms thin walled structure theory, areas and shell elements are used while preparing finite element model. Furthermore, the material used in the analyses is aluminum 6010.

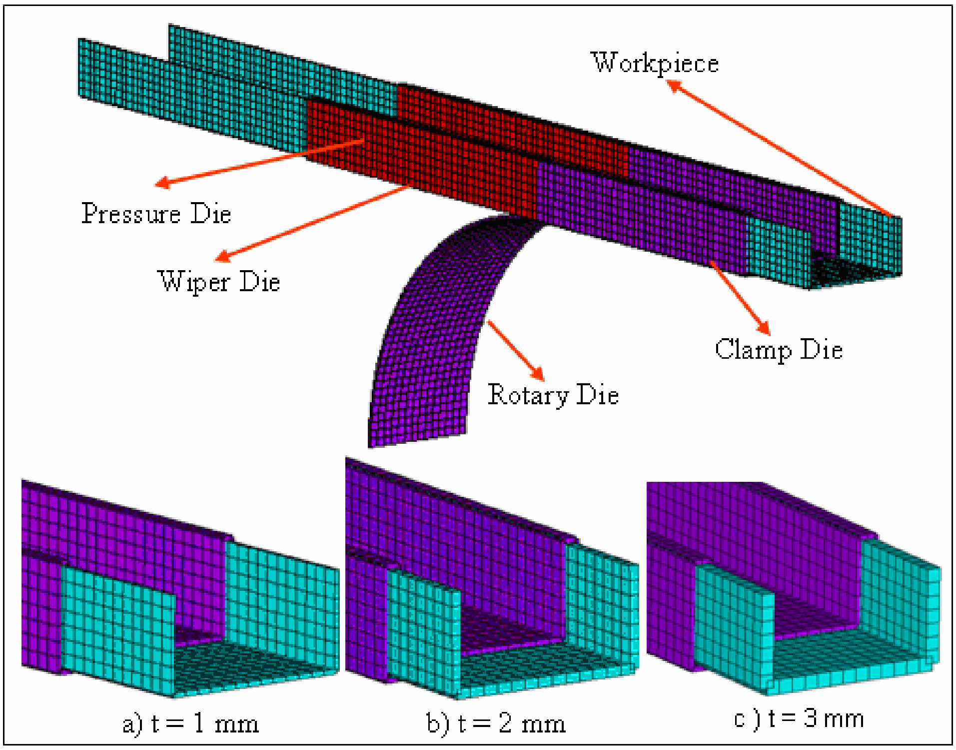

Figure 3.10 FEM for R=100 mm and a) t = 1 mm, b) t = 2 mm, c) t = 3 mm

3.2.2 Strains in Beams after Bending Operation

Simulation results show that the less bend radius used in the bending, the more strain beam has. Hence, the most critical bend radius of 100 mm is shown in details for the strain distribution investigation in Figure 3.11.

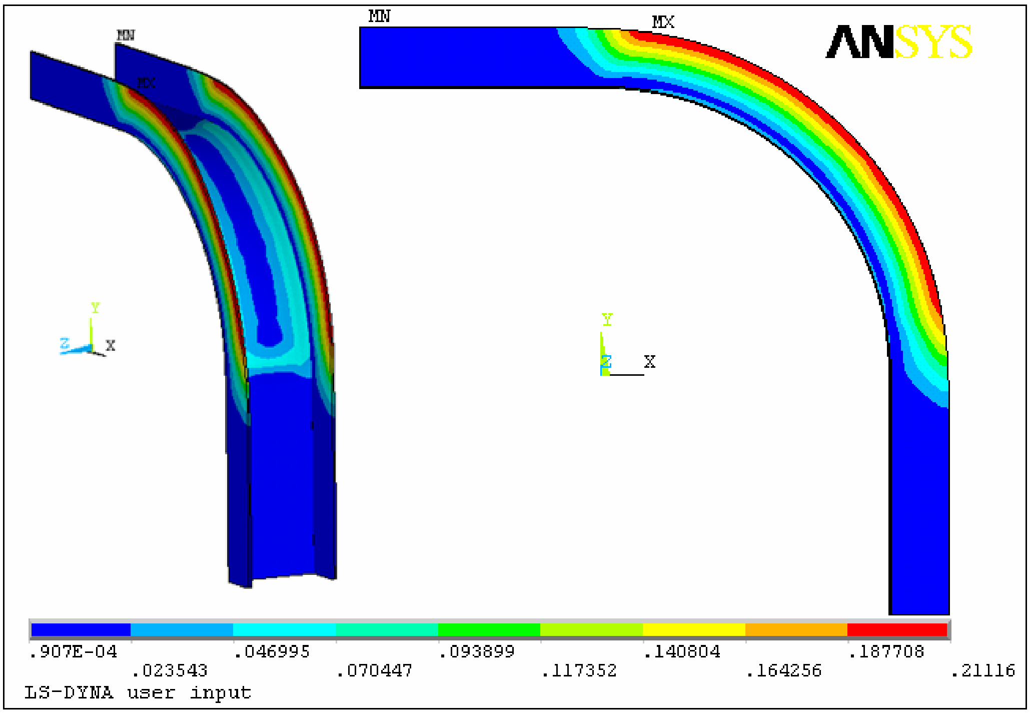

Figure 3.11 Total Equivalent Strain Distribution in Bent U-Shaped Beam for R=100 mm and t = 1 mm

As it can be seen from Figure 3.11, the beam has maximum total equivalent strain of 0.211 approximately. Figure 3.12 verifies that when the bend radius increases the total equivalent strain decreases. Figure 3.12 is prepared for U-Shaped beams having wall thickness of 1 mm.

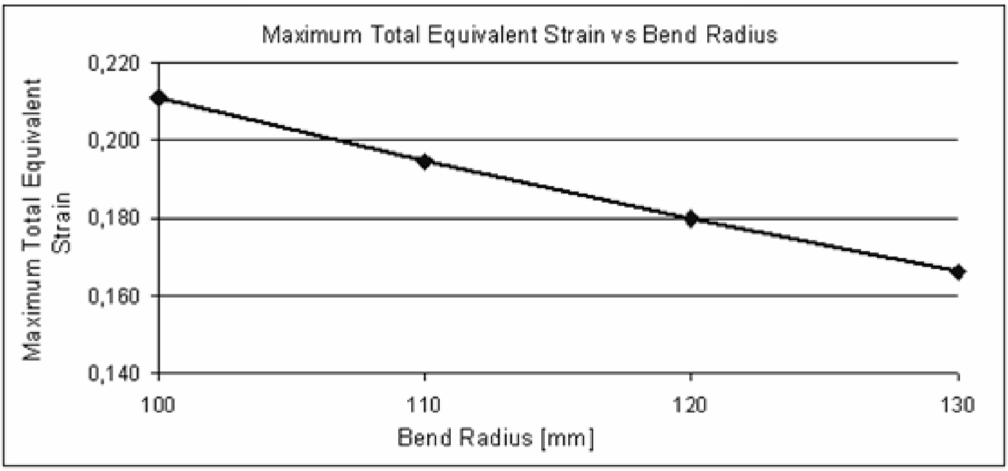

Figure 3.12 Max. Total Equiv. Strain Values wrt. Various Bend Radius for t =1 mm

3.2.3 Wall Thickness Change after Bending Operation

The effect of tensile stress at the outer side is thinning and the effect of compressive stress at the inner side is thickening (Figure 3.13). Moreover, as it can be seen from Figure 3.12, the strain values are decreasing with the increasing bend radius. Therefore, the thinning phenomenon is decreasing with increasing bend radius and decreasing strain values (Figure 3.14).

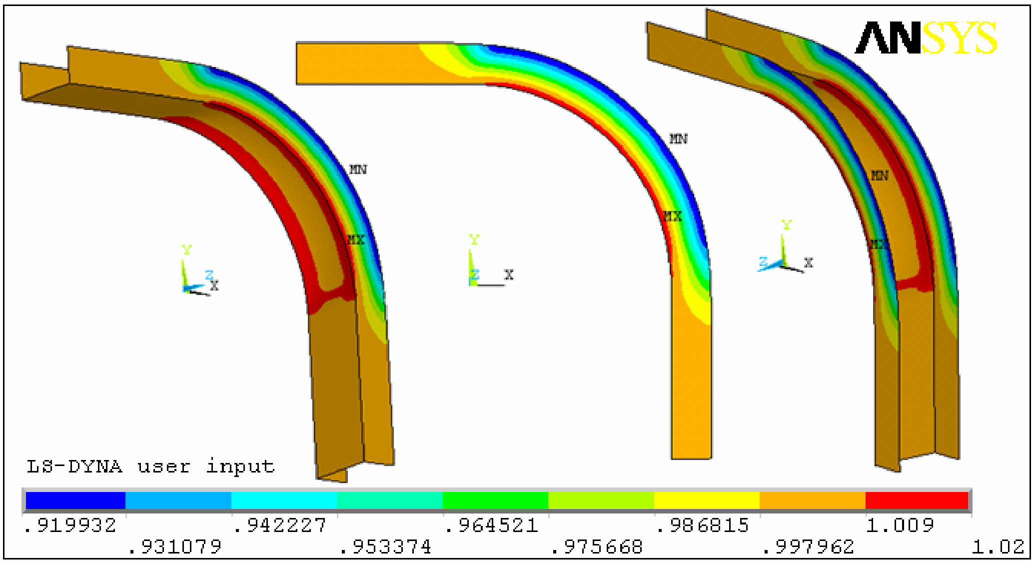

Figure 3.13 Wall Thickness Distribution in Bent U-Shaped Beam, R=100mm, t=1mm

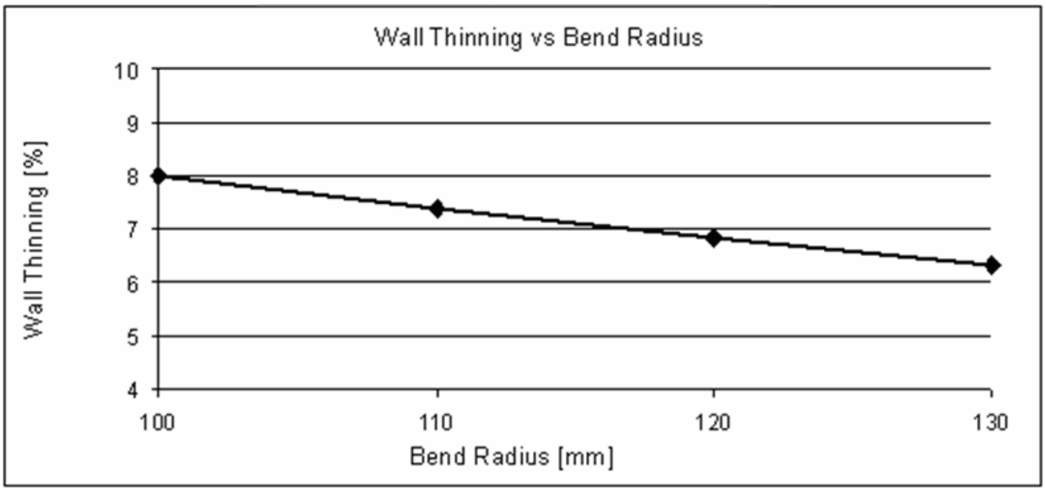

Figure 3.14 Wall Thinning With Respect To Various Bend Radius

Figure 3.13 shows the regions in compression as red and the regions in tension as blue; the red regions denote wall thickening, while the blue regions denote wall thinning. The maximum wall thinning change in U-shaped beam for bending radius of 100 mm and wall thickness of 1 mm is almost 8%. And this wall thinning values are decreasing linearly with the increasing bend radiuses.

3.2.4 Springback Behavior after Unloading

In this part, the springback behavior of beams is investigated (Figure 3.15), and the effects of bend radius and wall thickness on springback of U-Shaped beams are observed.

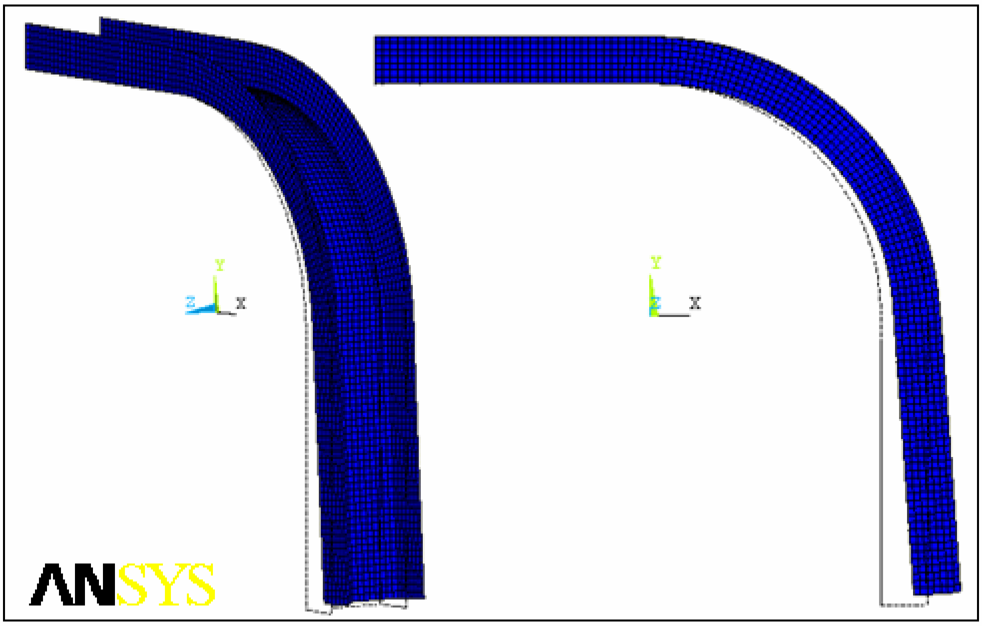

Figure 3.15 Springback of U-shaped Beam after Unloading, R=100 mm and t=1 mm

It has been observed that the strain values for smaller bend radiuses are higher. Therefore, the beams bent to smaller bend radiuses are strain-hardened more. This phenomenon causes the beams springback less than the beams bent to large bend radiuses. Figure 3.16 shows the springback angles with respect to various bend radiuses for various thicknesses.

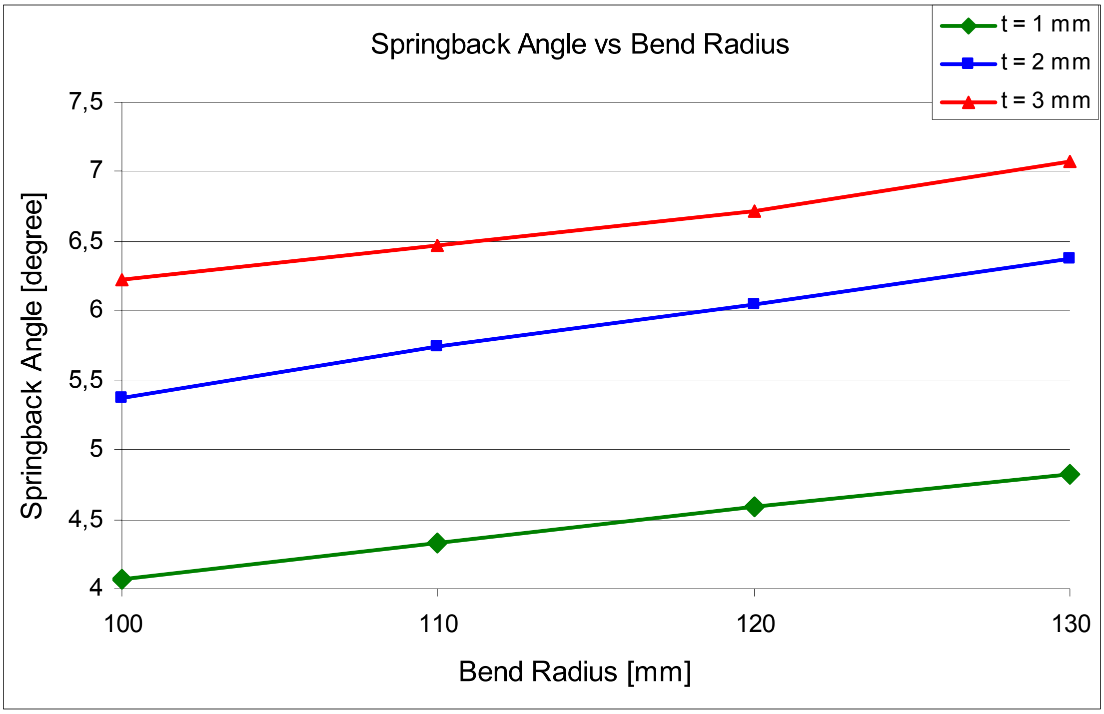

Figure 3.16 Springback Angle Comparison for Wall Thicknesses of 1,2 and 3 mm

When a line is fitted to scattered springback data, as it can be seen from Figure 3.16 that the trend lines can be assumed to be linear, and the equations of fitted lines are

$$\theta_{spring} = 0.0254R_{bend} + 1.534 \qquad \text{for } t = 1 \text{ mm}$$

$$\theta_{spring} = 0.0333R_{bend} + 2.058 \qquad \text{for } t = 2 \text{ mm}$$

$$\theta_{spring} = 0.0282R_{bend} + 3.382 \qquad \text{for } t = 3 \text{ mm}$$

where θ in degree and R in mm. These springback equations are specific for aluminum U-shaped beams having width of 40 mm, height of 20 mm.

All the model properties are kept constant during the analyses in order to examine the effect of wall thickness on springback. Under the same conditions, the springback angle difference is roughly 1.5^0 for the specific U-shaped beam dimensions having a=40 mm, b=20 mm and t=1 & 2 mm. The springback angle difference between 2 and 3 mm thick beams is roughly 0.8^0. As in T-shaped beam bending operations, the springback angles are increasing with increasing thickness values.

3.3 Bending Analyses of Tubular Beams With Respect To Various Bend Radius and Wall Thickness

Since tubular beams are most commonly used beam types in manufacturing field, wall thickness change and springback angle issues become important. The aim of the analyses is to determine the wall thickness change over the circumference and springback behavior after unloading of tooling in rotary draw bending. In the analyses, the results of springback angle and wall thickness change are prepared for various bend radius and various wall thickness. Furthermore, a comparison between analytical method, finite element method and experimental results is managed for prediction of wall thickness change after bending process. According to comparison, it is seen that wall thickness prediction in FEA has a good agreement with the analytical method results and experimental results.

3.3.1 Finite Element Analysis

12 different analyses are performed for bending simulations of tubular beams with respect to changing bend radiuses and wall thicknesses as shown below.

- Bend radius, R = 70 mm for t = 1, t = 2, t = 3, t = 3.5 and t = 4 mm.
- Bend radius, R = 80 mm for t = 1, t = 2, t = 3, t = 3.5 and t = 4 mm.
- Bend radius, R = 90 mm for t = 1, t = 2, t = 3, t = 3.5 and t = 4 mm.
- Bend radius, R = 100 mm for t = 1, t = 2, t = 3, t = 3.5 and t = 4 mm.

The detailed results are shown in following titles only for bend radius of 70 mm and wall thickness of 1 mm. The varying parameters in the analyses are bend radius starting from 70 mm to 100 mm with 10 mm increments and wall thicknesses of 1, 2, 3, 3.5 and 4 mm. Figure 3.17 shows the cross-sectional details of tubular beam used in the analyses. The beams have a tube radius of 10 mm and wall thicknesses of 1, 2, 3, 3.5 and 4 mm. Figure 3.18 shows the finite element model for bend radius of 70 mm and wall thicknesses of 1, 2, 3, 3.5 and 4 mm. The material properties and element type used in tubular rotary draw bending simulation are the same as used in T and U shaped beam analyses (Aluminum 6010 and Shell 163).

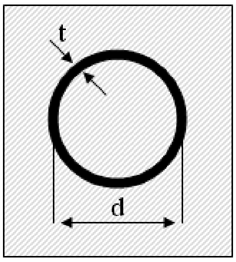

Figure 3.17 Cross-Section Details of Tubular Beam

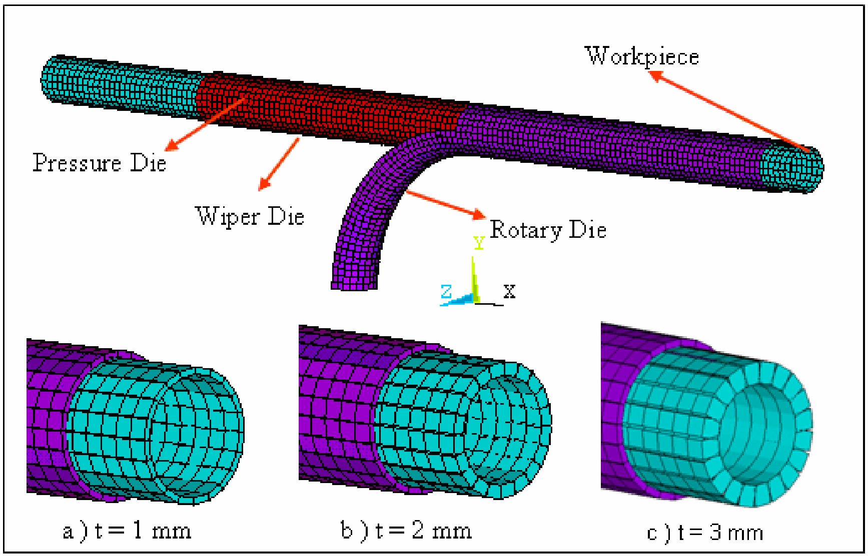

Figure 3.18 FE Model for R=70 mm and a) t=1 mm, b) t=2 mm, c) t=3mm

3.3.2 Strains in Beams after Bending Operation

As in T and U-shaped beams, the maximum strain value obtained from analyses belongs to beam which is bent to smallest bend radius (Figure 3.19). In tubular beam bending simulations, the beam radiuses used are 70, 80, 90 and 100 mm. Therefore, 70 mm bend radius, the most critical value, is given in details.

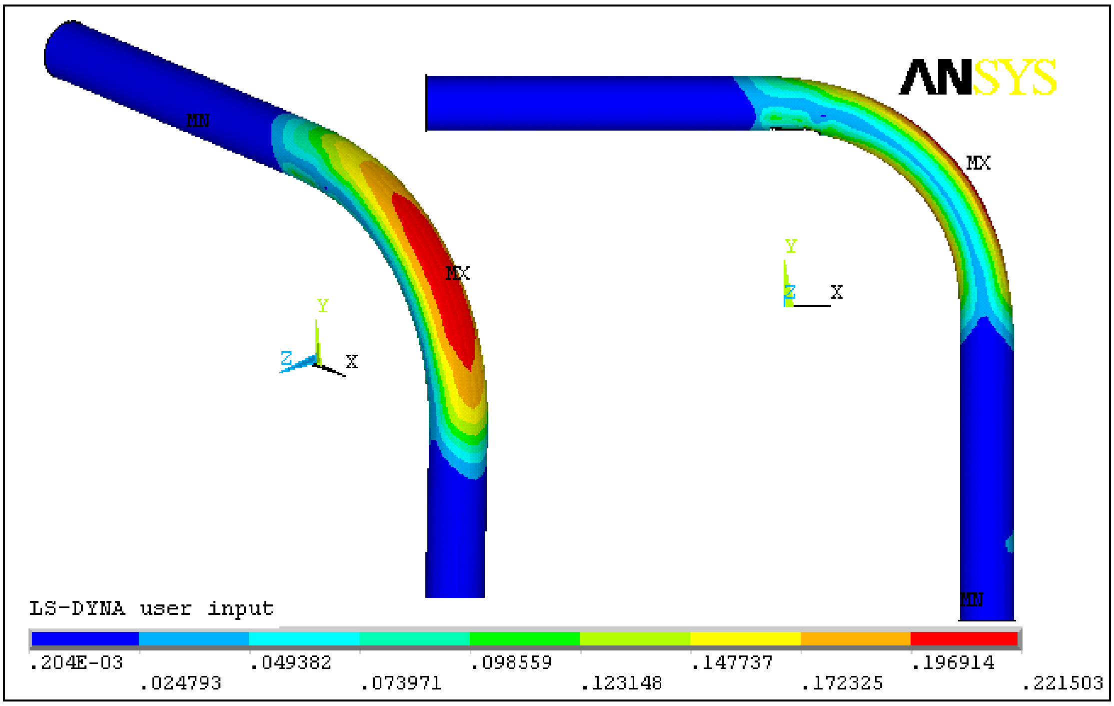

Figure 3.19 Total Equivalent Strain Distribution in Bent Tubular Beam for R=70 mm and t = 1 mm

For the smallest bend radius, the maximum equivalent strain value is the highest among all bend radiuses. Therefore, the strain values have a decreasing tendency with respect to increasing bend radiuses as shown in Figure 3.20.

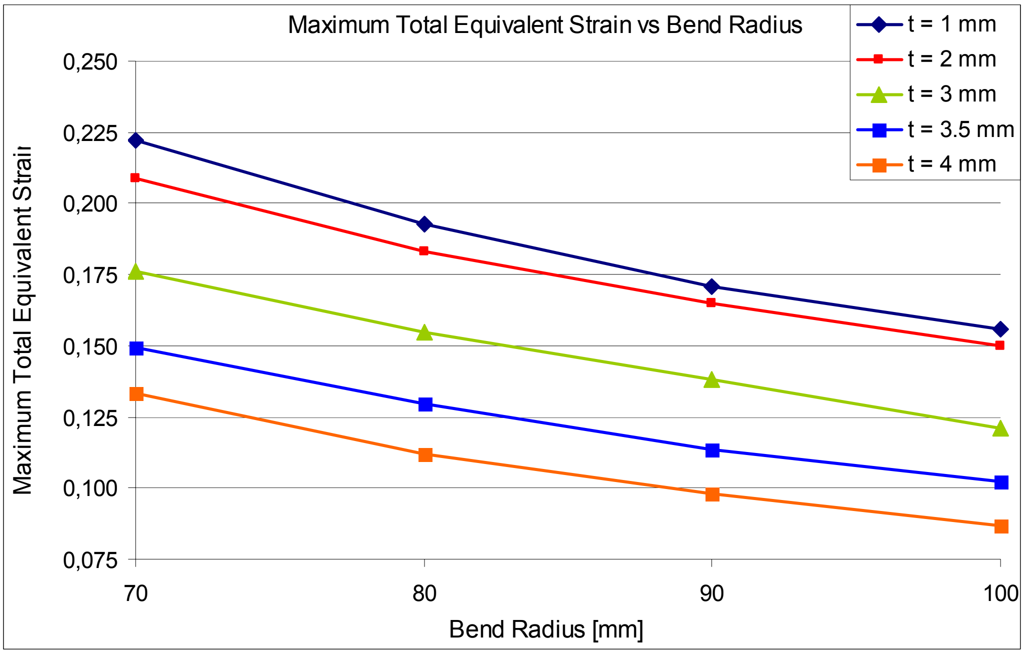

Figure 3.20 Max. Total Equiv. Strain Values With Respect to Various Bend Radius

3.3.3 Wall Thickness Change after Bending Operation

The common forming problem in rotary tube bending is the wall thinning at the extrados because of tensile stress induced (Figure 3.22). This thinning increases with increasing strain values. Figure 3.21 shows that the wall thinning decreases with increasing bend radius as in T and U shaped beam bending simulations.

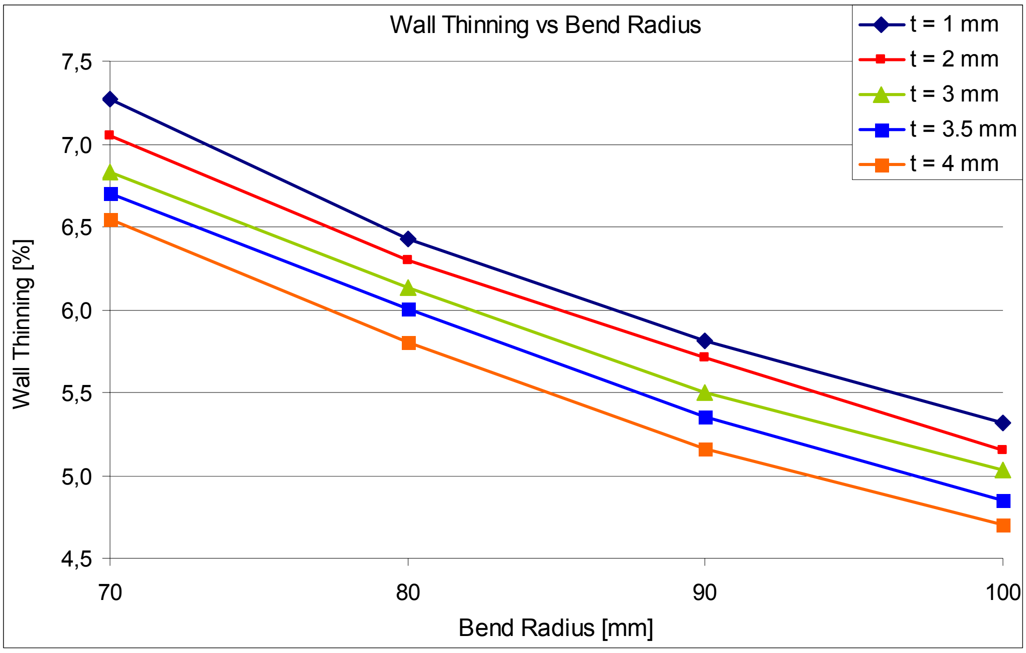

Figure 3.21 Wall Thinning With Respect To Various Bend Radius

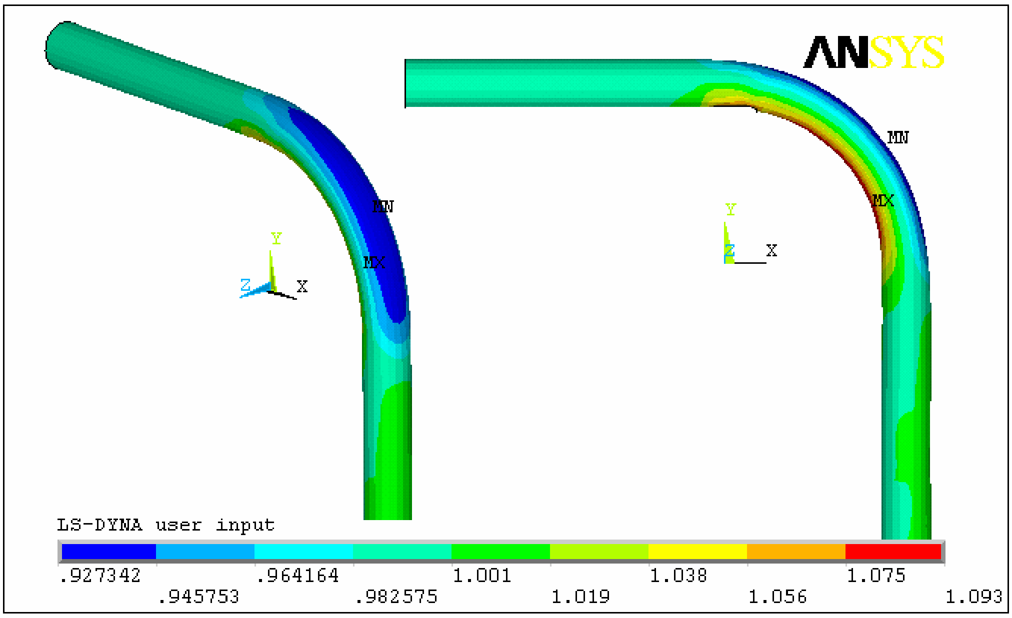

Figure 3.22 Wall Thickness Distribution in Bent Tubular Beam, R=70mm, t=1mm

The maximum wall thinning phenomenon occurs at where the maximum tensile stress exists, the outermost point extrados. This wall thinning can be seen in Figure 3.22, the contours show the thinning areas in blue and thickening areas in red.

3.3.4 Springback Behavior after Unloading

In order to investigate the springback response of tubular beams with respect to various bend radius and wall thickness, 12 different finite element analyses are performed implicitly (Figure 3.23). In rotary draw bending operations, it is verified that when bend radius increases, the springback angles also increases, since the strain values are higher in operations using smaller bend radiuses.

Furthermore, the strain values are higher, when the beam thickness is 1 mm. Therefore, the beams having 1 mm thickness undergo more strain hardening, and this causes that the springback angles are higher in thicker beams as shown in Figure 3.24.

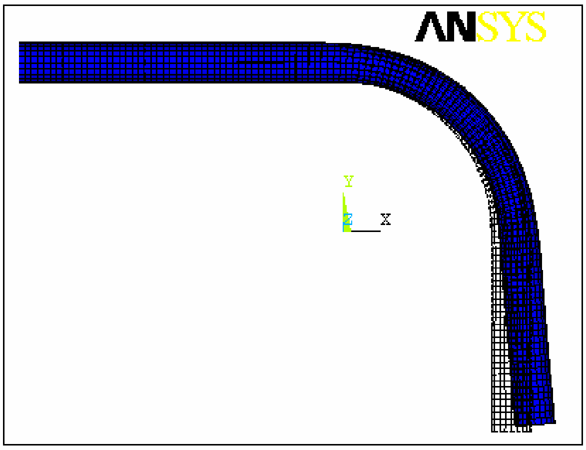

Figure 3.23 Springback of Tubular Beam after Unloading, R=70 mm and t=1 mm

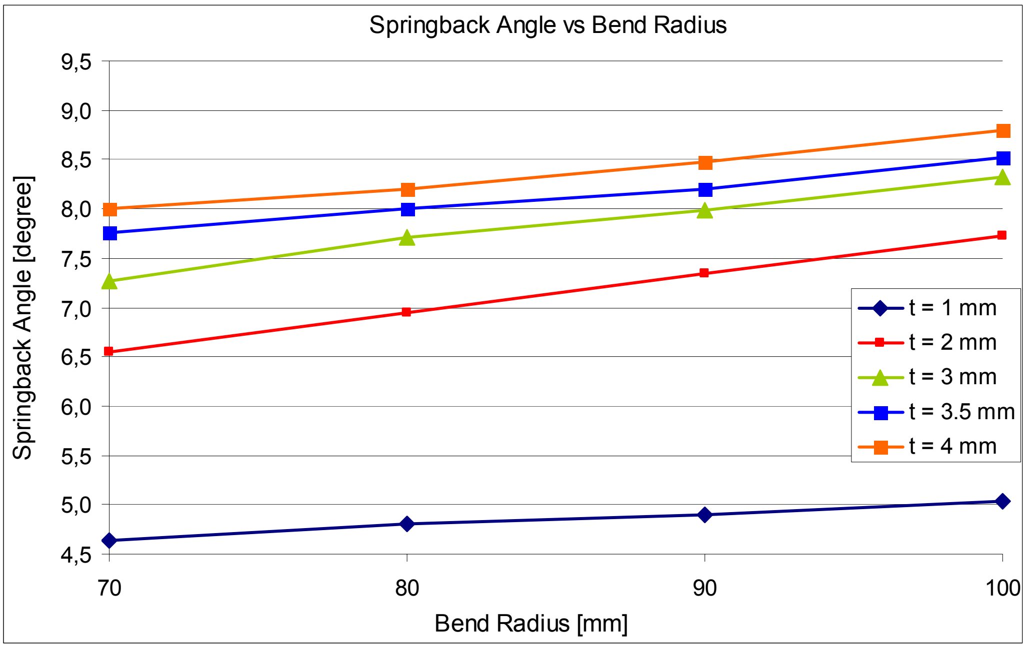

Figure 3.24 Springback Angle Comparison for Wall Thicknesses of 1, 2 and 3 mm

It is observed from the Figure 3.24 that when trend lines fitted to scattered data, the trend lines can be assumed linear. The fitted lines to the scattered data give the formulas where θ in degree and R in mm,

$$\theta_{spring} = 0.013R_{bend} + 3.735 \qquad \text{for } t = 1 \text{ mm}$$

$$\theta_{spring} = 0.039R_{bend} + 3.808 \qquad \text{for } t = 2 \text{ mm}$$

$$\theta_{spring} = 0.035R_{bend} + 4.879 \qquad \text{for } t = 3 \text{ mm}$$

$$\theta_{spring} = 0.025R_{bend} + 5.984 \qquad \text{for } t = 3.5 \text{ mm}$$

$$\theta_{spring} = 0.026R_{bend} + 6.115 \qquad \text{for } t = 4 \text{ mm}$$

By using these formulas, the springback angle can be predicted beforehand for this particular material and dimensions selected.

3.3.5 Experimental Results

The verification of bending simulation results are performed by comparing the springback angle and the thickness variation over circumference. In order to perform these verifications, tubes having 20 mm diameter and 1 mm thickness are used. The test setup is shown in Figure 3.25.

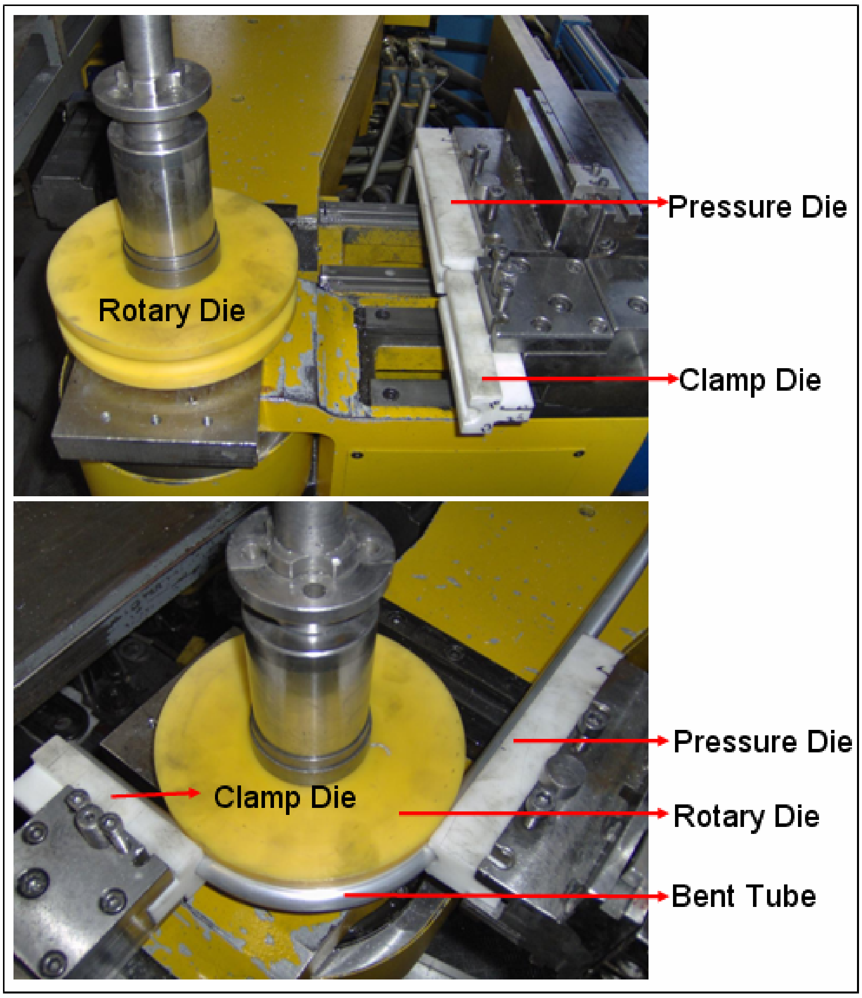

Figure 3.25 Test Setup Used for Verification of Bending Simulation Results

It has been observed from simulations that the springback angle of bent tube having 20 mm diameter and wall thickness of 1 mm is 5.03^0. After bending of several tubes, average springback angle is found as 5.22^0 in the tests. Figure 3.26 shows the springback angle comparison of simulation results and experimental results.

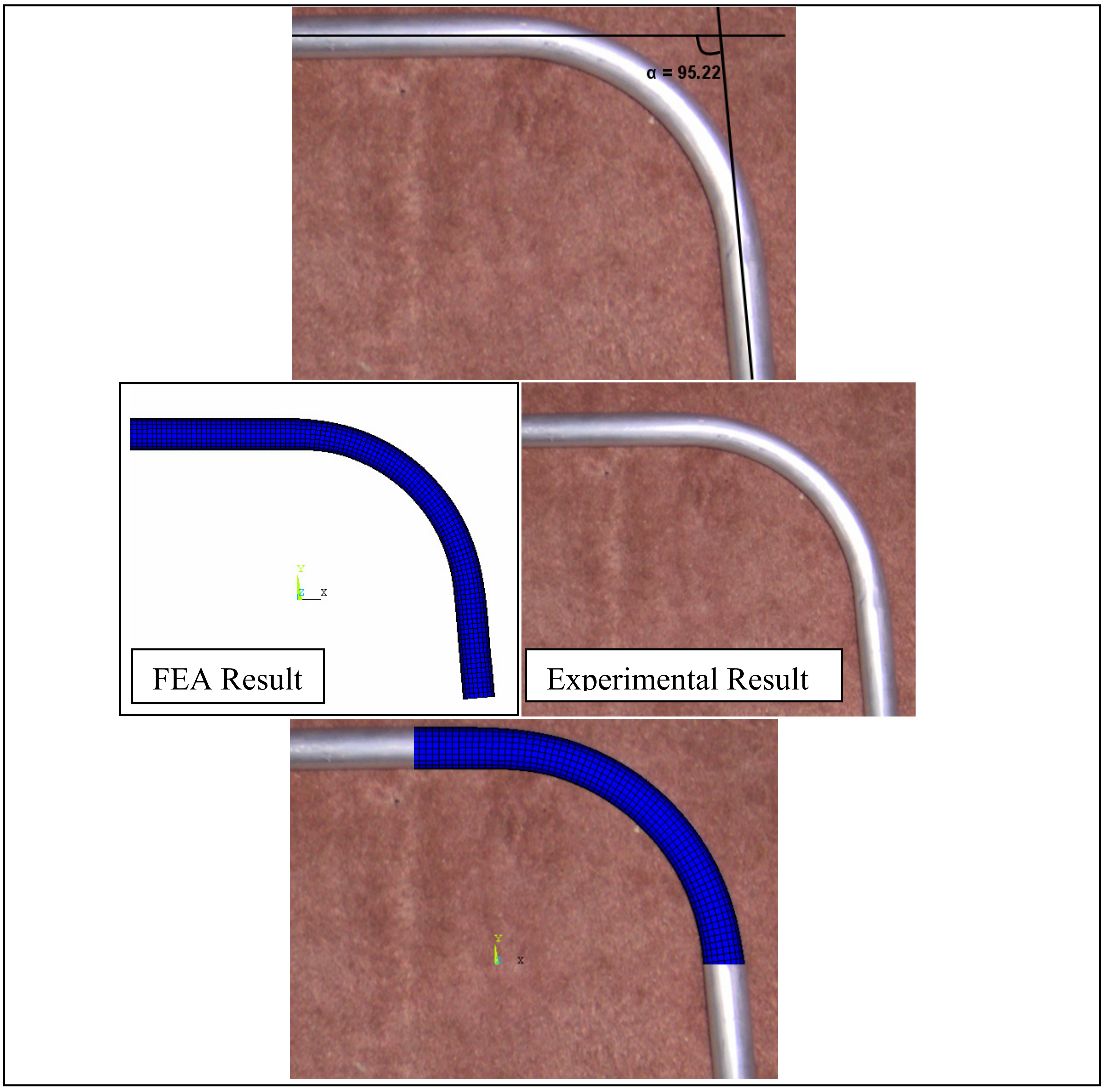

Figure 3.26 Springback Comparison of Simulation and Experimental Results

Tang [13] has developed an analytical method to predict wall thickness values over circumference. The results calculated with Tang's formulas, obtained from finite element analyses and test are as seen in Figure 3.29. The thickness values calculated by Tang's formula, extracted from analyses and experiments are for cut plane shown in Figure 3.27, and the cross-section distortion obtained by FEA and experimental results are shown in Figure 3.28.

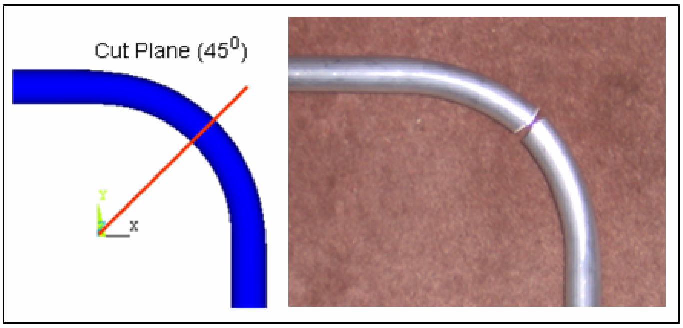

Figure 3.27 Cut Plane

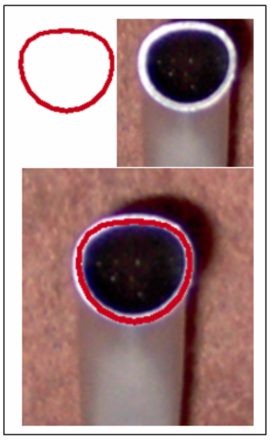

Figure 3.28 Cross Section Comparison of Simulation and Experimental Results

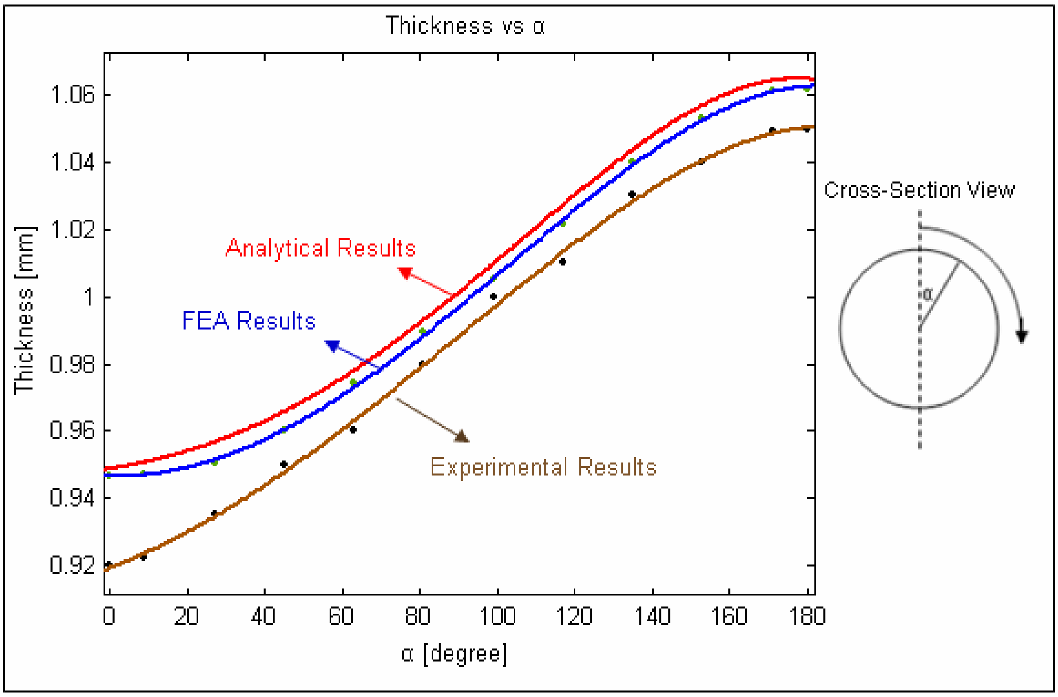

Figure 3.29 Wall Thickness Values Over Circumference for Tubular Beam

3.4 Bending Analyses of Tubular Beams With Respect To Various Bend Angles

In previous sections, rotary draw bending simulations of different types of beams (T, U and Tubular) are performed for various bend radius and wall thickness. This section deals with a specific type of tubular beam and constant dimensional values.

In all previous analyses the bend angle is 90^0. In this section, the aim is to obtain a relation between different bend angles and springback angles. According to where beams are used, the bend angles may change. A beam can be needed to be bent to different angles. However, the springback angles should be known to bend the beam to a desired angle, as the springback angles differ for various bend angles.

In this section, a tubular aluminum beams having bend radius of 100 mm and wall thicknesses of 1, 2, and 3 mm are bent to different angles ranging from 10^0 to 90^0 with 5^0 increments. The springback angles for each bend angle are found and a line is fitted to those scattered data. The equation of line is used to predict springback angle and even the overbend angle can be predicted from the equation.

3.4.1 Finite Element Analysis

In order to have a scattered data of springback values for different bend angles, 17 analyses are performed for each thickness value in which bend angle varies from 10^0 to 90^0 degrees with 5^0 increments.

The cross-sectional dimensions are chosen from standard catalogues such that the diameter of the tube is 20 mm and wall thicknesses are 1, 2 and 3 mm as shown in Figure 3.30.

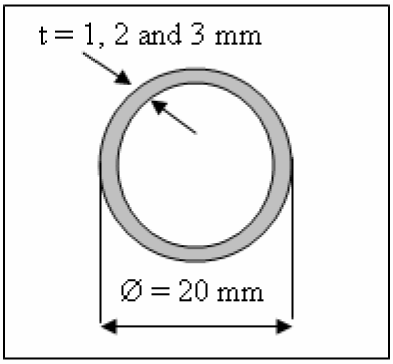

Figure 3.30 Cross-Section Details of Tubular Beam

The model is prepared as shown in Figure 3.18. The rotary draw bending tooling has a bend radius of 100 mm. In all previous finite element analyses, the rotational displacement load is applied to rotary die such that the die rotates 90^0 (~1.57 rad.) around its center. However, in this model, the load is applied to rotary die with 5^0 increments.

3.4.2 Strains in Beams after Bending Operation

As experienced from previous beam bending simulations, the maximum equivalent strain is obtained at the outermost point (extrados) and also the location of maximum strain is almost in half of bend angle. Figure 3.31 shows the strain distribution on tubular beams bent to 30^0, 60^0 and 90^0, and Figure 3.32 shows the maximum equivalent strain values with respect to bend angles. As it can be seen from Figure 3.32, the maximum strain values have a positive decreasing tendency.

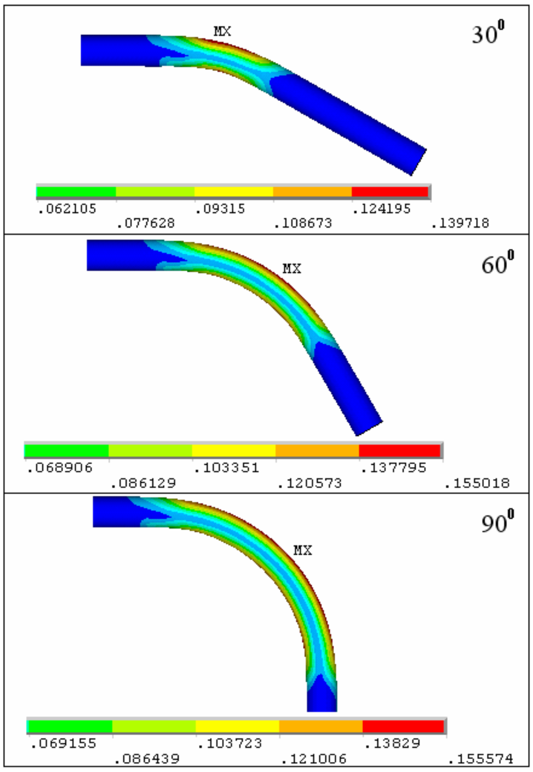

Figure 3.31 Total Equivalent Strain Distribution of 1 mm Thick Profile for 30^0, 60^0 and 90^0 Bend Angles

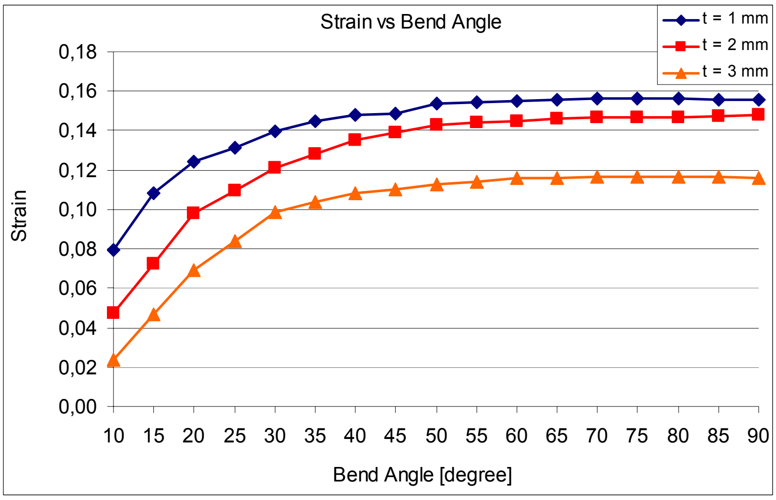

Figure 3.32 Max. Tot. Equiv. Strain Values of 1,2 and 3 mm Thick Profiles for Various Bend Angles

3.4.3 Springback Behavior after Unloading

While the beam is bent to different bend angles, the springback angles are changing for those bend angles (Figure 3.34). The springback behavior of tubular beam has a linear increasing tendency, although the strain values in the beam increase. In previous sections, it has been experienced that while strain values increase, the springback angles decrease because of strain hardening phenomenon. However, in this application the results are different. After bending operation, the portion in the beam that causes springback has an important role. Since the deformed portion of the beam increases with increasing bend angles, the relaxation portion increases. Therefore, the portion causing springback increases and springback angles increase with increasing bend angle as shown in Figure 3.33.

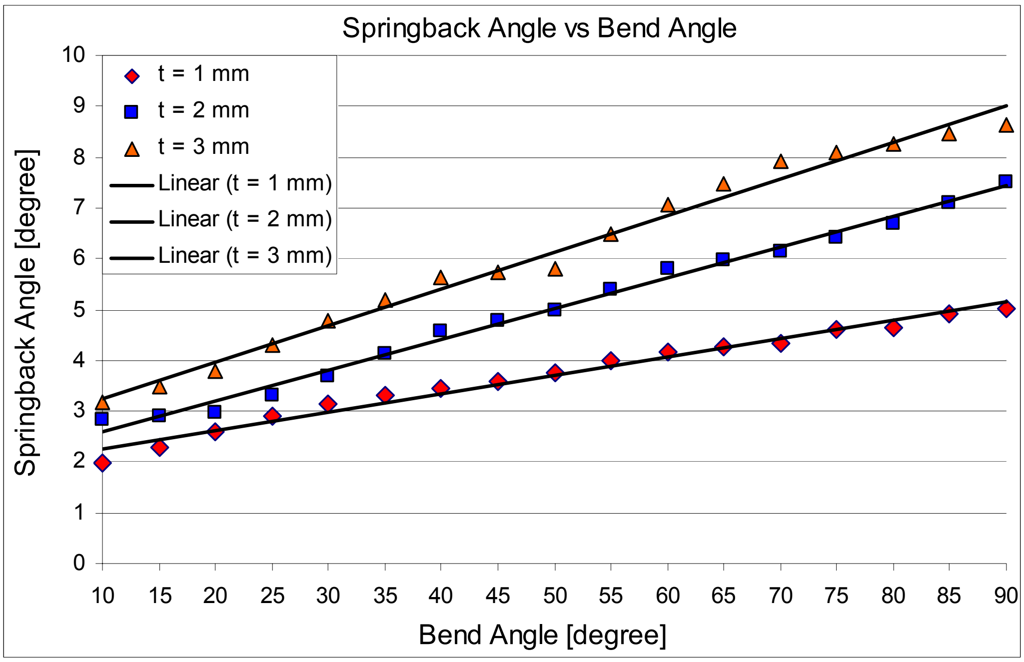

Figure 3.33 Springback Angle with Respect to Bend Angle for Tubular Profiles

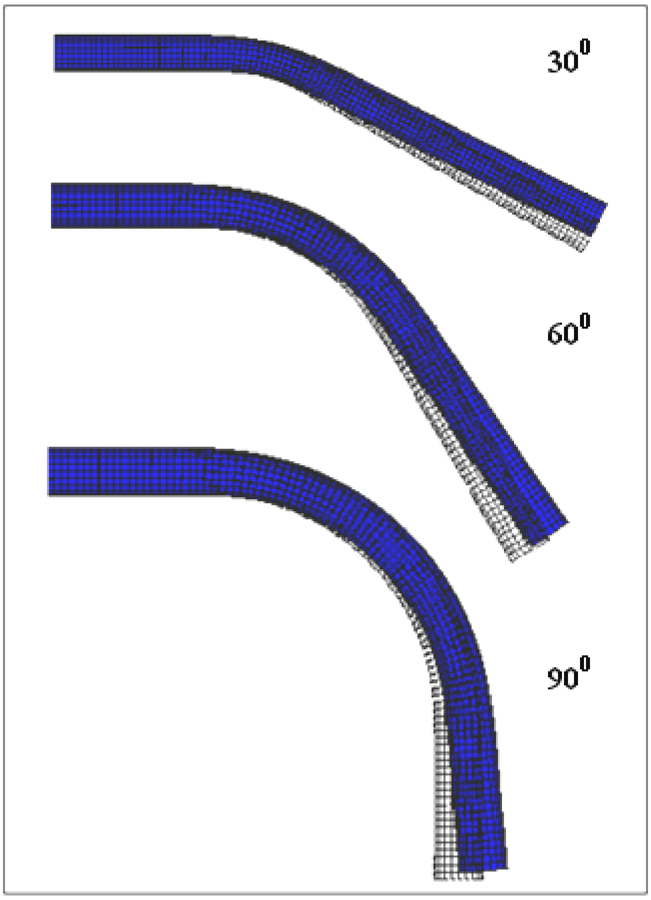

Figure 3.34 Springback of Beams for 30^0, 60^0 and 90^0 Bend Angles

If a curve is fitted to scattered data, the curve is nearly straight and its equation is $\theta_{springback} = 0.03590\theta_{bend} + 1.9094$ for t = 1 mm. This equation can be used to predict overbend angle which compensate springback angle for desired bend angle. However, this equation can only be used for this specific tube dimensions, bend radius and material type.

If θ_{bend} is the bend angle that compensates the springback angle.

$$\theta_{bend} = \theta_{desired} + \theta_{springback} , \quad (6)$$

The springback angle equation extracted from Figure 3.33 is as follows.

$$\theta_{springback} = 0.0359\theta_{bend} + 1.9094, \tag{7}$$

By substituting eqn. (6) into eqn. (7),

$$\theta_{bend} - \theta_{desired} = 0.0359\theta_{bend} + 1.9094\ , \tag{8}$$

It is found that,

$$\theta_{bend} = 1.037\theta_{desired} + 1.98, \text{ for t = 1 mm} \tag{9}$$

$$\theta_{bend} = 1.064\theta_{desired} + 2.11, \text{ for t = 2 mm} \tag{10}$$

$$\theta_{bend} = 1.078\theta_{desired} + 2.72, \text{ for t = 3 mm} \tag{11}$$

Finally, Eqn.9, 10 and 11 can be used to predict overbend angle for a desired bend angle for this specific tubular beam for various thicknesses.

After 17 finite element analyses, springback angle values are extracted from each analysis, and a curve is fitted to these scattered data, the resulting curve can be assumed to be linear for each thickness value. By the help of this linear curve, the springback angle values can be predicted for a given bend angle. Furthermore, this springback equation is used to find overbend angle for a given desired bend angle as given in Eqn.9, 10 and 11.

3.5 Bending Analyses of Tubular Beams with Additional Loadings

In all previous analyses, the models are prepared such that the only load in models was rotational displacement applied to rotary die. In this chapter, the aim is to investigate the effects of additional loadings on bent tubes which are axial pull and internal pressure.

The aim of applying axial pull is to reduce the springback of beams after unloading. Since axial pull causes stretching of beams, the maximum strain values at the extrados increase. Therefore, the beams undergo more strain hardening, and finally the springback values decrease.

The cross-sectional distortion is the common problem of tubular beams after bending operations. Internal pressure gives a resisting internal force to tubular beams so that the ovality problem is overcome. However, in this case, the beam faces with another problem which is excessive thinning at the extrados due to circumferential stress resulted from internal pressure. Another thing that should be taken into account is fracture. If the internal pressure applied is so high, the beam can fail.

3.5.1 Axial Pull

In previous analyses, the models are prepared such that the ends of beams were free to move in longitudinal direction. In this case, the models are prepared exactly as the same in previous analyses except that the beams are fixed at their ends near pressure die.

With this additional load, the springback behavior of the beams is examined with respect to various bend radius and wall thickness. The bend radiuses are chosen as 70, 80, 90, 100 mm. Furthermore, the beams have wall thicknesses of

1 and 2 mm. Figure 3.35 shows the finite element model prepared for this application.

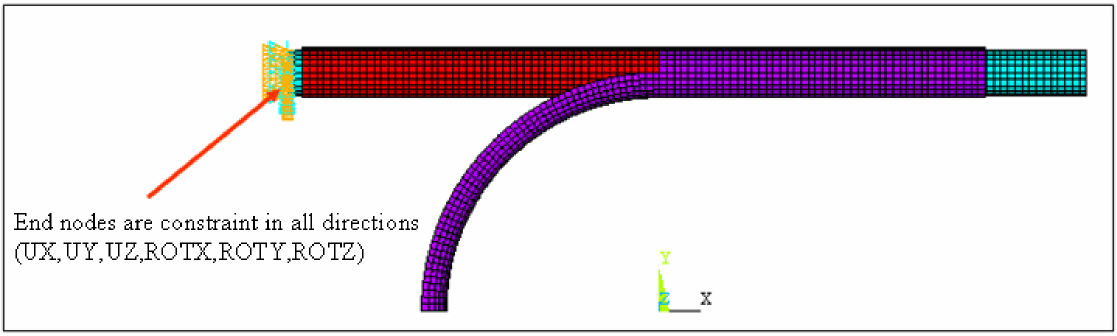

Figure 3.35 Finite Element Model for R = 100 mm

The beam is fixed at its end near pressure die. If the beam is long, the beam elongates along the length and the stretching cannot be preformed properly. Therefore, the length of the beam is kept short so that the beam is stretched during bending operation.

It was experienced that when wall thickness is increased, the springback angles increase for the similar beams under the same conditions. Moreover, as it is mentioned before, when the beam is fixed at its end, the springback values decrease. Figure 3.36 and Figure 3.37 show this situation for a tubular beam having 10 mm beam radius, 70, 80, 90 and 100 mm bend radiuses and 1 & 2 mm wall thicknesses.

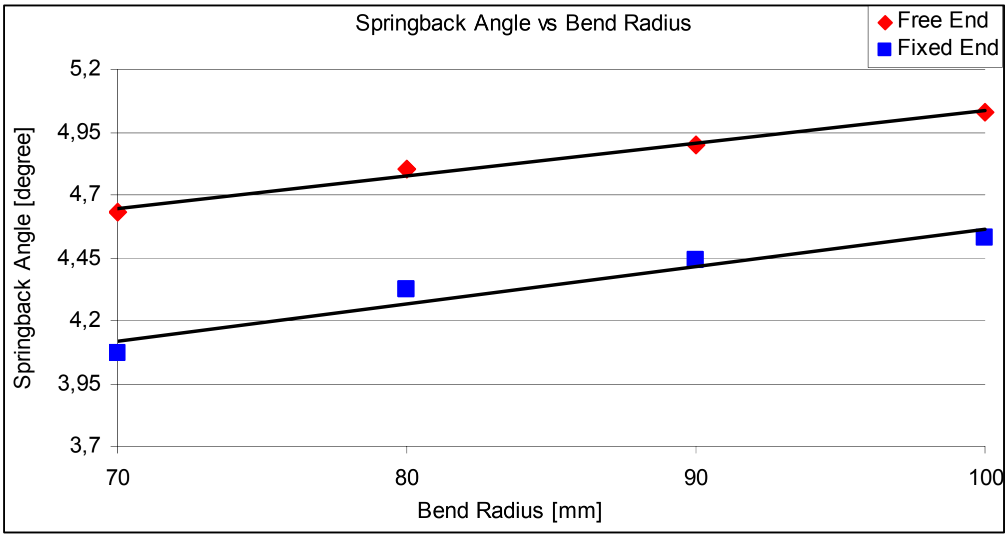

Figure 3.36 Springback Angle Comparison of Fixed and Free Beams Having Wall Thickness of 1 mm With Respect to Various Bend Radius

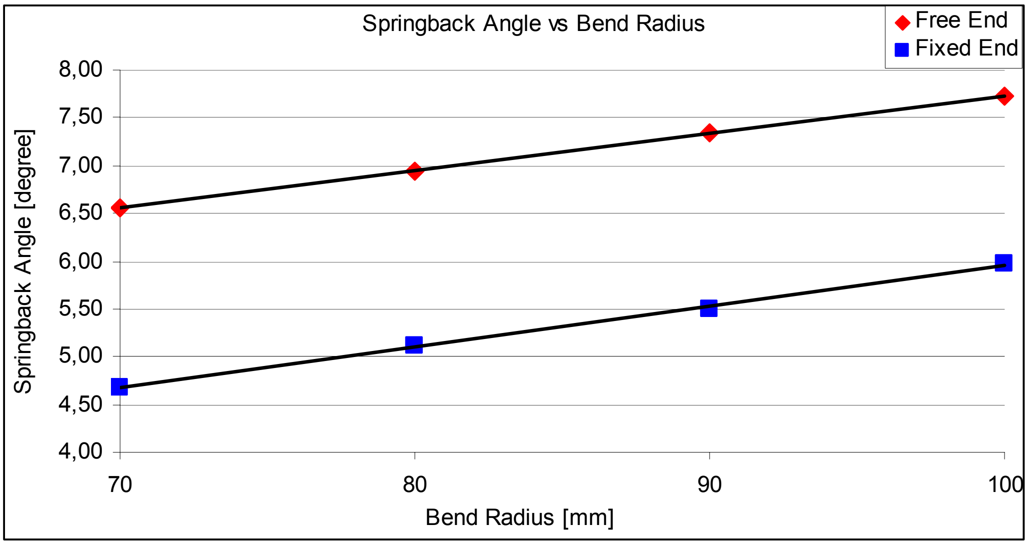

Figure 3.37 Springback Angle Comparison of Fixed and Free Beams Having Wall Thickness of 2 mm With Respect to Various Bend Radius

Since the strain values increase, when the beams are fixed, springback angles decrease as it can be seen from Figure 3.36 and Figure 3.37. The reduction in springback angle for t = 1 mm is almost 0.5^0, while the reduction in springback angle for t = 2 mm is almost 1.8^0.

3.5.2 Internal Pressure

In rotary draw tube bending operations, the most commonly problem faced is flattening of tube. When a tube is bent to a desired angle over a desired bend radius, the cross-section of the tube changes its shape to oval (Figure 3.38).

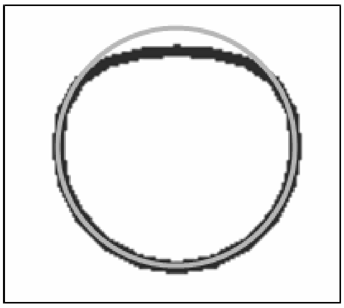

Figure 3.38 Cross-Section of Tube after Bending

Since the beam is weak to resist for collapsing of outer surface, the outer surface of the tube flattens and the cross-section shape cannot be kept as it was before. There are several parameters affecting flattening phenomenon which are wall thickness, tube radius, bend radius, bend angle etc. However, in this section, all of those parameters are kept constant. The model has a tube radius of 10 mm, wall thickness of 1 mm, bend radius of 80 mm and bend angle of 90^0. While preparing finite element model, the additional load is applied to tube. The internal pressure is applied to overcome cross-section distortion problem (Figure 3.39).

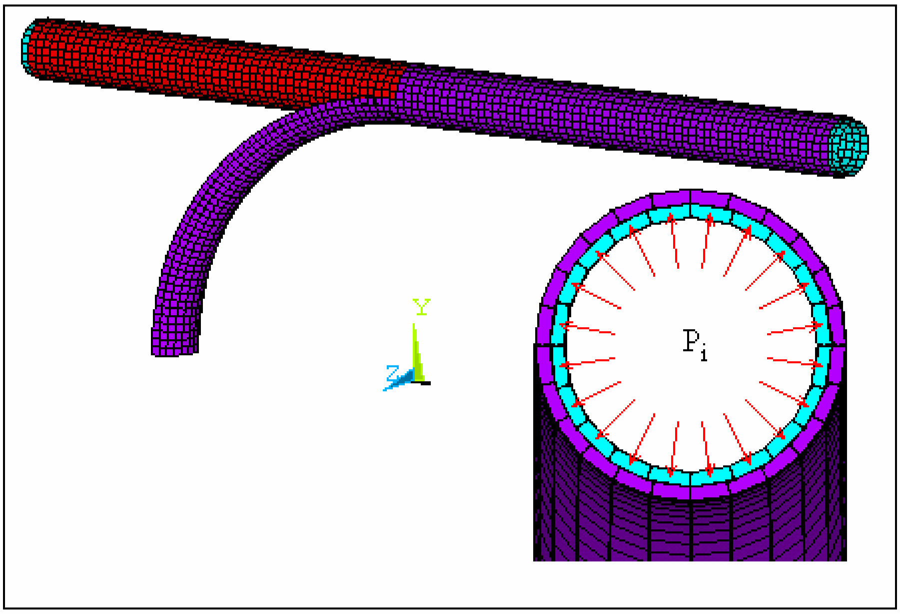

Figure 3.39 Finite Element Model of Rotary Draw Tube Bending With Internal Pressure

In order to see the effect of internal pressure, the same model is used for each analysis except that the internal pressures are changing. Firstly, a model is prepared just for bending operation without any internal pressure. Then, 2.5, 5, 7.5 and 10 MPa internal pressures are applied respectively.

Since the internal resistance of tube is increased with increasing internal pressure, the cross-section shapes are recovered and the flattening of the tube decreases as shown in Figure 3.40.

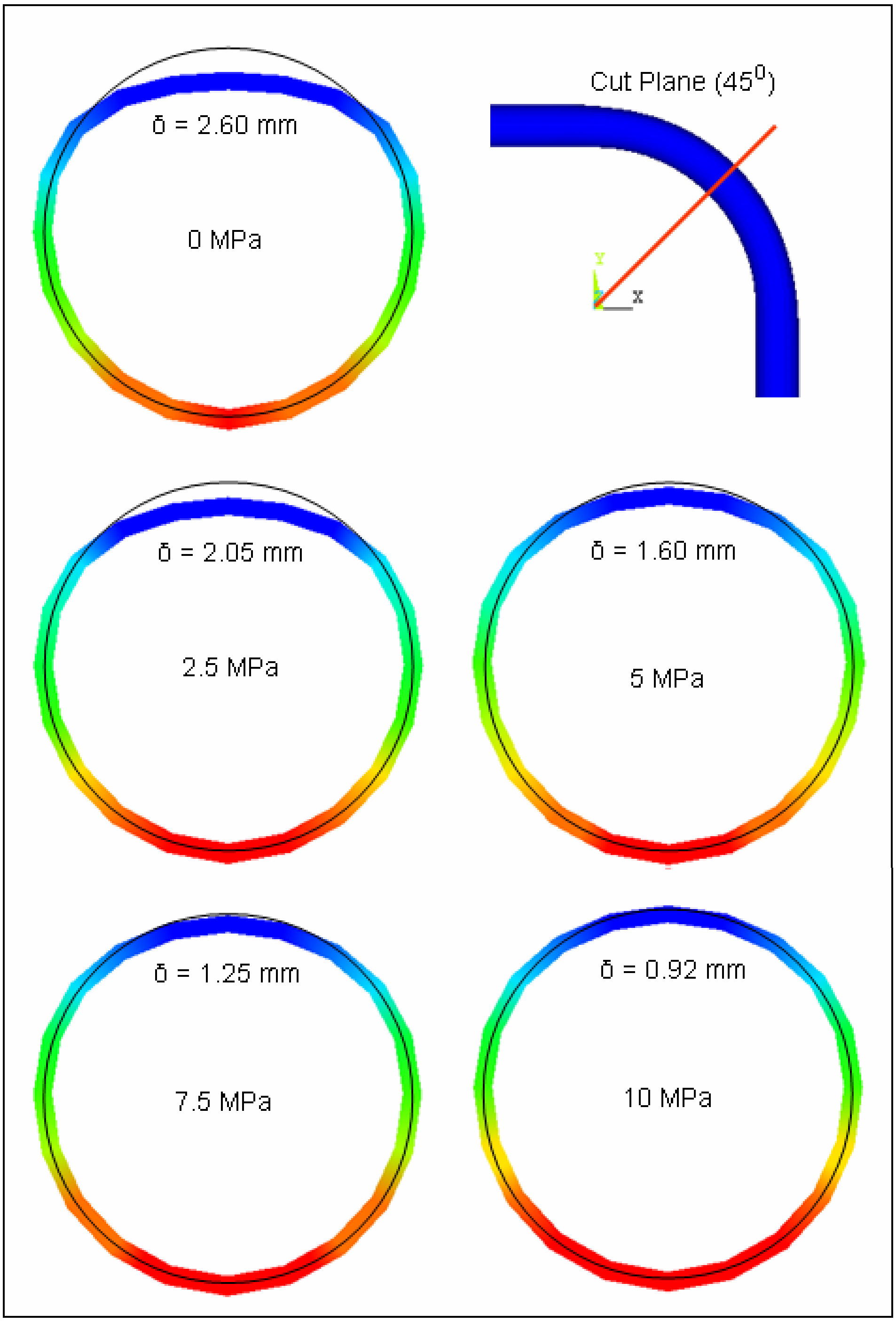

Figure 3.40 Cross-Section Details of Beams For Different Internal Pressures

Since the maximum strain value is obtained at 45^0 cut plane, all data is taken from that cross-section. As shown in Figure 3.40, when the internal pressure increases, the flattening (δ) value decreases. If no internal pressure is applied, the maximum flattening value at the outermost point is 2.60 mm. While the pressure is increased to 2.5 MPa, the cross- section is a little bit recovered and the flattening becomes 2.05 mm. If the pressure applied is increased to 10 MPa, the minimum flattening value can be obtained. The relationship between internal pressure and flattening of tube is given in Figure 3.41 below.

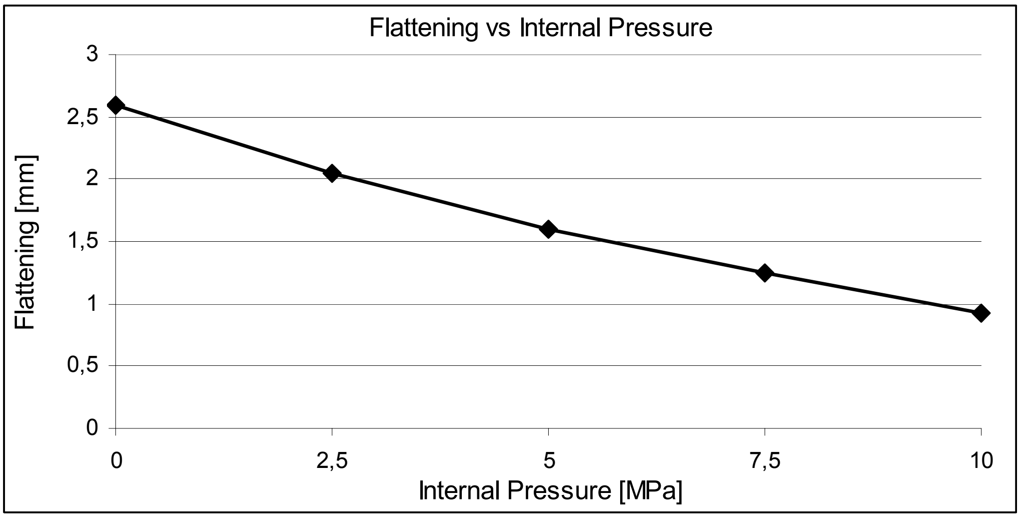

Figure 3.41 Flattening of Tube With Respect to Internal Pressure

As it can be seen from Figure 3.41, there is nearly a linear relationship between internal pressure and flattening. This internal pressure can be increased such that the flattening phenomenon is overcome. However, in this case, strain value should be taken into account. Since the internal pressure makes the tube expand in radial direction, the strain values increase in the tube, and this strain values must be below level of fracture. Figure 3.42 shows the maximum equivalent strain values with respect to internal pressure.

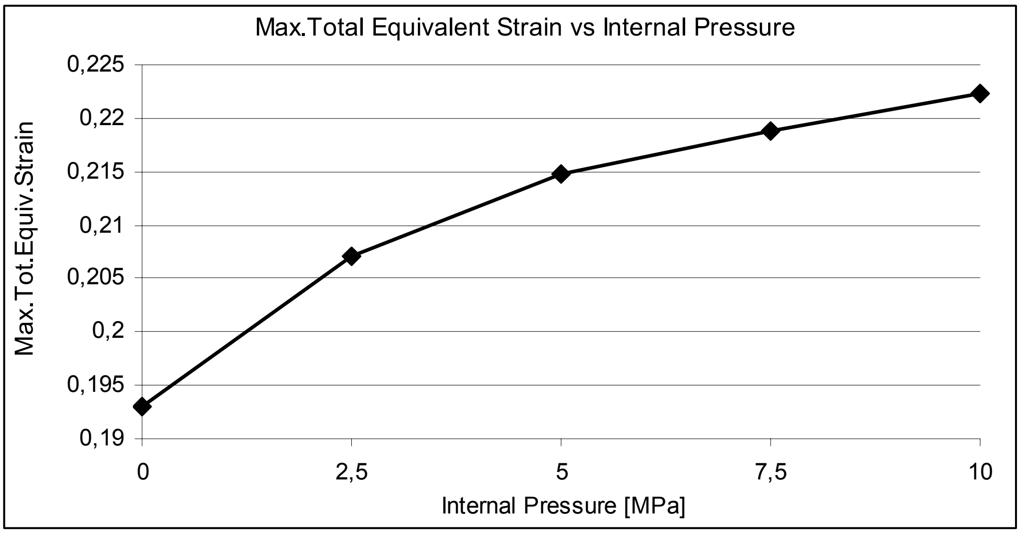

Figure 3.42 Max. Tot. Equiv. Strain Values With Respect to Internal Pressure

It can be seen from Figure 3.42 that the maximum strain value increases with increasing internal pressure. If the internal pressure is increased to have zero flattening, the tube most probably fails, since the fracture strain of beam is exceeded.

Another issue in applying internal pressure is excessive thinning at the extrados. Since the strain at the extrados increases, the thinning ratio at the outer surface increases as shown in Figure 3.43. Beside this, it is known that when a tube is bent, the thickening occurs at the inner side. Application of internal pressure also decreases this thickening phenomenon (Figure 3.44).

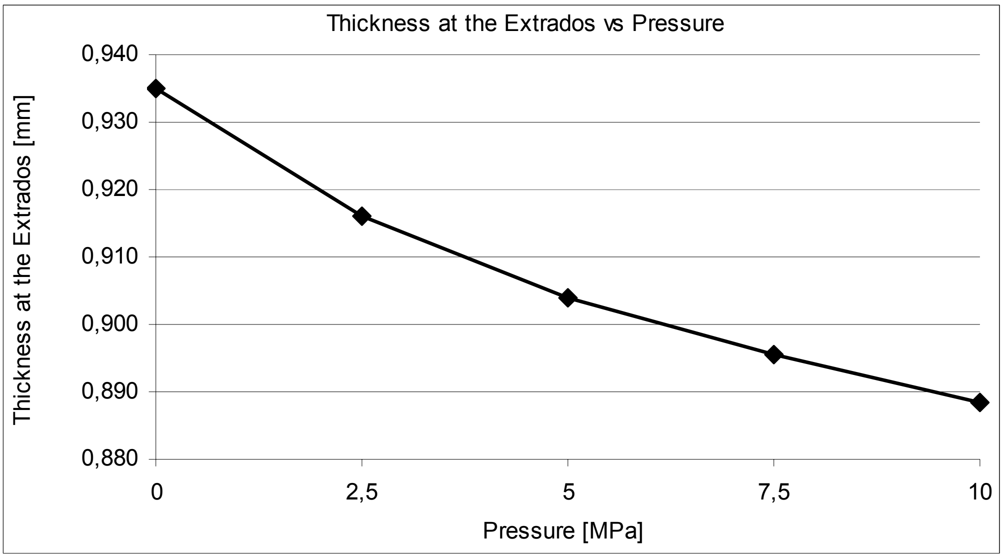

Figure 3.43 Min. Thickness Values at Extrados With Respect to Internal Pressure

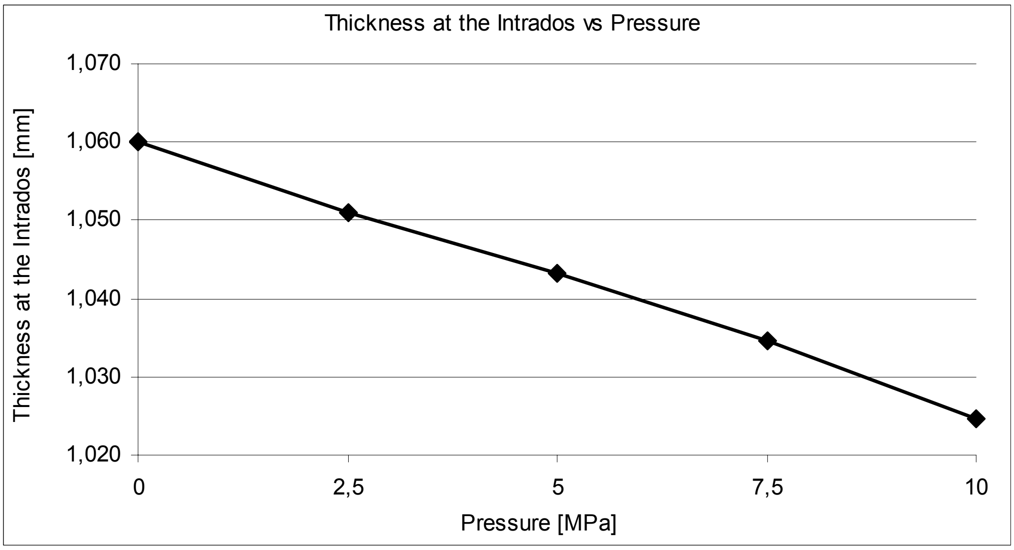

Figure 3.44 Max. Thickness Values at Intrados With Respect to Internal Pressure

Figure 3.43 and Figure 3.44 show the thickness values at extrados and intrados respectively. The thinning change at the extrados increases from almost 6.4% to 11.1%. Furthermore, the thickening ratio at the intrados decreases from almost 6.2% to 2.5%.

Figure 3.45 shows the wall thickness values of tube over its circumference, and the cut plane is in the middle of bent portion of tube (see Figure 3.27) When the internal pressure increases, the thickness values at all points decrease. There exists an offset between thickness lines. However, this offset decreases around 100^0. Because the neutral axis of tube is shifted down during bending operation, and the thickness values around neutral axis do not change much.

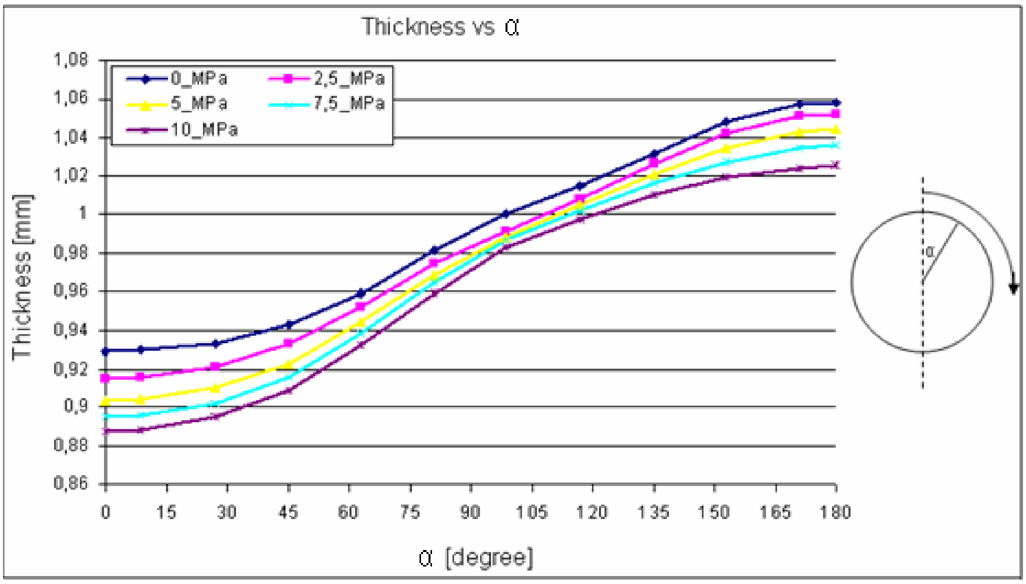

Figure 3.45 Wall Thickness Values Over Circumference

In conclusion, the main purpose of applying axial pull is to reduce springback angle after unloading. When the additional axial load is applied to end of tube, the tube is stretched during bending operation. Therefore, the strain values on the tube increase. The increase in strain values causes the material strain hardened more, and the material strength of the tube is also increased. Then the springback values of tubes whose one end is fixed are reduced compared to tubes whose ends are free.

The other additional loading is internal pressure applied to inner side of tube during bending operation. By applying internal pressure, the cross-section distortion problem can be overcome. Since the thin walled tube cannot resist to collapsing of outer surface, the flattening phenomenon occurs. Addition of internal pressure provides extra internal resistance and the flattening can be avoided.

However, application of internal pressure causes another problem which is excessive thinning. Since the internal pressure makes the strain values increase on the tube, the thickness values at the extrados decrease. Furthermore, the internal pressure makes the tube expand in radial direction, and the strain values increase.

CHAPTER 4

CONCLUSIONS

The main aim of this study is to investigate springback behavior and cross-section distortions of some commonly used beam types with respect to various bend radius, wall thickness, and bend angles by using finite element method. The following conclusions are drawn from the study.

1. Bending of T-shaped and U-shaped beams to 90^0 :
   (a) The results showed that in bending processes, the outer side undergoes tensile stress, while the inner side is in compression. This causes thinning at the outer side, and thickening at the inner side.
   (b) The amount of springback increases linearly with increasing bend radius. When the bend radius increases, the maximum strain in the beam decreases. Therefore, the material undergoes less strain hardening and the beam springs back more.
   (c) The effect of increased wall thickness is the increase in springback angles.

2. Bending of tubular beams to 90^0 :
   (a) It is shown that the springback angles of tubular beams increase linearly with the increasing bend radius.
   (b) Comparison of wall thickness variation showed that finite element analyses results, analytical method results, and experimental results are in good agreement.

3. Bending of tubular beams to different angles :
   (a) A linear relation is obtained between the bend angle and springback angle (Figure 3.33) for various wall thicknesses.

4. Bending operations with additional loading,
   (a) It is observed that the axial pull reduces springback angles. As a result of increasing strain and hence strain hardening. Therefore, the springback angles of the beam decreases.
   (b) Internal pressure provides internal resistance which reduces flattening phenomenon. The results showed that when the internal pressure increases, the cross-section of the tube is mostly recovered. However, when high internal pressure is applied, an excessive thinning occurs at the outer side (extrados) of the tube and the strain values get higher. Therefore, the internal pressure should be applied such that the tube is kept in safe region, below fracture strain, otherwise the beam fails.

REFERENCES

1. Zhan, M.; Yang, H.; Jiang, Z.Q.; Zhao, Z.S.; Lin, Y.: A Study on a 3D FE Simulation Method of the NC Bending Process of Thin-Walled Tube, Journal of Materials Processing Technology, 129 (2002), pp. 273-276.

2. Kim, J.; Kang, S.J.; Kang, B.S.: Computational Approach to Analysis and Design of Hydroforming Process for an Automobile Lower Arm, Computer And Structures, 80 (2002), pp. 1295-1304.

3. Stelson, K.A.; Lou, H.: Three Dimensional Tube Geometry Control for Rotary Draw Tube Bending Part1:Bend Angle and Overall Tube Geometry, Journal of Manufacturing Science and Engineering, 123 (2002), pp. 258-265.

4. Jin, Z.; Luo, S.; Daniel, F.X.: KBS-Aided Design of Tube Bending Processes, Engineering Applications of Artificial Intelligence, 14 (2001), pp. 599-606.

5. Semiatin, S.M.: Forming and Forging Volume 14-9th Edition Metals Handbook, ASM International, (1988), pp. 1499-1451.

6. Yang, J.B.; Jeon, B.H.; Oh, S.: The Tube Bending Technology of a Hydroformig Process for an Automotive Part, Journal of Materials Processing Technology, 111 (2001), pp. 175-181.

7. The Principles of Tube Bending, *Retrieved* 02.09.2007, *from* Summo Manufacturing: http://www.summo.com/technology.htm.

8. Miller, J.E.; Kyriakides, S.; Bastard, A.H.: On Bend-Stretch Forming of Aluminum Extruded Tubes-I Experiments, International Journal of Mechanical Sciences, 43 (2001), pp. 1283- 1317.

9. Arild, H.C.; Odd, S.H.; Magnus, L.: Stretch Bending of Aluminum Extrusions for Car Bumpers, Journal of Materials Processing Technology, 102 (2000), pp. 241-248.

10. Zhan, M.; Yang, H.; Huang, H.; Gu, R.: Springback Analysis of Numerical Control Bending of Thin Walled Tube Using Numerical-Analytic Method, Journal of Materials Processing Technology, 117 (2006), pp. 197-201.

11. Yang, H.; Lin, Y.: Wrinkling Analysis for Forming Limit of Tube Bending Processes, Journal of Materials Processing Technology, 152 (2004), pp. 363-369.

12. Brazier, L.Z.: On the Flexure of Thin Cylindrical Shells and Other Thin Sections, Proceedings of the Royal Society of London, 116 (1927), pp.104-114.

13. Tang, N.C.: Plastic-Deformation Analysis in Tube Bending, International Journal of Pressure Vessels and Piping, 77 (2000), pp. 751-759.

14. Lee, H.; Van Tyne, C.J.; Field, D.: Finite Element Bending Analysis of Oval Tubes Using Rotary Draw Bender for Hydroforming Applications, Journal of Material Processing Technology, 168 (2005), pp. 327-335.

15. Zeng, Y.; Li, Z.: Experimental Research on the Push-Bending Process, Journal of Material Processing Technology, 122 (2002), pp. 237-240.

16. Gao, L.; Strano, M.: FEM Analysis of Tube Pre-Bending and Hydroforming, Journal of Material Processing Technology, 151 (2004), pp. 294-297.

17. Wang, J.; Agarwal, R.: Tube Bending Under Axial Force and Internal Pressure, Journal of Manufacturing Science and Engineering, 128 (2006), pp. 598-605.

18. Oral, S., *ME 404 Thin Walled Structures, Lecture Notes*. 2006: METU, Ankara.

19. Mechanical Properties of Aluminum, *Last Accessed Date* April.01.2008, *from* Material Property Data: http://www.matweb.com/search/SpecificMaterial.asp?bassnum=MA6010T4.

20. ANSYS 11.0, *Documentation for ANSYS*, *Chapter 2.4*. 2007.

APPENDIX A

CODES FOR PREPARING FINITE ELEMENT MODEL OF T-SHAPED BEAM

In this appendix, APDL [20] (ANSYS Parametric Design Language) codes are given for T-Shaped beam having wall thickness of 2 mm and bend radius of 130 mm.

Table A.1: Finite Element Model for T-Shaped Beams, R=130 mm and t=2 mm

	FLST,2,8,4,ORDE,2
/Prep7	FITEM,2,4
K,1,-250,0,0	FITEM,2,-11
K,2,-250,0,10	ADRAG,P51X, , , , , , 12
K,3,-250,0,-10	FLST,2,3,4,ORDE,3
K,4,-250,19.5,0	FITEM,2,1
L,1,2	FITEM,2,3
L,1,3	FITEM,2,13
L,1,4	ADRAG,P51X, , , , , , 13
K,5,0,1.5,10.5	LDELE, 13, , ,1
K,6,0,-1.5,10.5	K,30,200,0,-10
K,7,0,-1.5,-10.5	L,30,3
K,8,0,1.5,-10.5	L,30,25
K,9,0,1.5,-1.5	FLST,2,4,4
K,10,0,20,-1.5	FITEM,2,2
K,11,0,20,1.5	FITEM,2,32
K,12,0,1.5,1.5	FITEM,2,35
L,5,6	FITEM,2,13
L,6,7	AL,P51X
L,7,8	K,50,0,1.5,10.5
L,8,9	K,51,0,-1.5,10.5
L,9,10	K,52,0,-1.5,-10.5
L,10,11	K,53,0,1.5,-10.5
L,11,12	K,54,0,1.5,-1.5
L,12,5	K,55,0,20,-1.5
K,13,175,0,0	K,56,0,20,1.5
K,14,0,0,0	K,57,0,1.5,1.5
K,15,200,0,0	L,50,51
L,14,13	L,51,52
L,1,15	L,52,53
L,55,56	L,53,54

Table A.1 Continued

L,56,57	L,54,55
L,57,50	*SET,_RC_SET,2,
K,58,-250,0,0	R,2
L,14,58	RMODIF,2,1, , ,1, , , ,
FLST,2,8,4,ORDE,2	*SET,_RC_SET,3,
FITEM,2,36	R,3
FITEM,2,-43	RMODIF,3,1, , ,1, , , ,
ADRAG,P51X, , , , , , 44	MAT,1,
FLST,3,19,5,ORDE,2	MPREAD,'3_param_Barlat','SI_MPL',' ',LIB
FITEM,3,1	MPLIST,1
FITEM,3,-19	TBLIST,ALL,1
!Bend Radius	EDMP,RIGI,2,7,4
AGEN, ,P51X, , , ,130, , , ,1	MP,DENS,2,7.85e-9
K,80,0,0,100	MP,EX,2,2e5
FLST,2,2,4,ORDE,2	MP,NUXY,2,.3
FITEM,2,12	*CSET,1,2, 2,3,
FITEM,2,44	MPCOPY, ,2,3
LDELE,P51X, , ,1	TBCOPY,ALL,2,3
K,85,0,0,0	EDMP,RIGI,3,7,7
FLST,2,1,4,ORDE,1	MPDE,DENS,3
FITEM,2,5	MP,DENS,3,7.85E-009
FLST,8,2,3	MPDE,EX,3
FITEM,8,85	MP,EX,3,2E+005
FITEM,8,80	MPDE,NUXY,3
AROTAT,P51X, , , , , ,P51X, ,90, ,	MP,NUXY,3,0.3
APLOT	FLST,2,20,5,ORDE,2
FLST,5,9,5,ORDE,3	FITEM,2,1
FITEM,5,1	FITEM,2,-20
FITEM,5,-8	AESIZE,P51X,3,
FITEM,5,20	CMSEL,S,PROFILE
ASEL,S, , ,P51X	FLST,5,3,5,ORDE,2
CM,Rotary_Die,AREA	FITEM,5,9
FLST,5,8,5,ORDE,2	FITEM,5,-11
FITEM,5,12	CM,_Y,AREA
FITEM,5,-19	ASEL, , , ,P51X
ASEL,S, , ,P51X	CM,_Y1,AREA
CM,Sabit_Die,AREA	CMSEL,S,_Y
FLST,5,3,5,ORDE,2	CMSEL,S,_Y1
FITEM,5,9	AATT, 1, 1, 1, 0,
FITEM,5,-11	CMSEL,S,_Y
ASEL,S, , ,P51X	CMDELE,_Y
CM,Profile,AREA	CMDELE,_Y1
ALLSEL,ALL	MSHAPE,0,2D
ET,1,SHELL163	MSHKEY,1
ET,2,SHELL163	FLST,5,3,5,ORDE,2
ET,3,SHELL163	FITEM,5,9
*SET,_RC_SET,1,	FITEM,5,-11
R,1	CM,_Y,AREA
RMODIF,1,1, ,5,2, , , ,	ASEL, , , ,P51X
CMSEL,S,_Y	CM,_Y1,AREA

Table A.1 Continued

AMESH,_Y1	CHKMSH,'AREA'
CMDELE,_Y	CM,_Y1,AREA
CMDELE,_Y1	CHKMSH,'AREA'
CMDELE,_Y2	CMSEL,S,_Y
CMSEL,S,ROTARY_DIE	AMESH,_Y1
FLST,5,9,5,ORDE,3	CMDELE,_Y
FITEM,5,1	CMDELE,_Y1
FITEM,5,-8	CMDELE,_Y2
FITEM,5,20	ALLSEL,ALL
CM,_Y,AREA	EDPART,CREATE
ASEL, , , ,P51X	EDCGEN,ASSC, , ,0.1,0.1,0,0,0, , , , ,0,10000000,0,0
CM,_Y1,AREA	*DIM,time,ARRAY,2,1,1, , ,
CMSEL,S,_Y	*DIM,deplas,ARRAY,2,1,1, , ,
CMSEL,S,_Y1	*SET,TIME(2,1,1) , 1.1
AATT, 2, 2, 2, 0,	*SET,DEPLAS(2,1,1) , -1.727
CMSEL,S,_Y	EDLOAD,ADD,RBRZ,0, 2,TIME,DEPLAS, 0, , , , ,
CMDELE,_Y	FLST,2,3,4,ORDE,2
CMDELE,_Y1	FITEM,2,1
FLST,5,9,5,ORDE,3	FITEM,2,-3
FITEM,5,1	/GO
FITEM,5,-8	DL,P51X, ,UY,
FITEM,5,20	FLST,2,3,4,ORDE,2
CM,_Y,AREA	FITEM,2,1
ASEL, , , ,P51X	FITEM,2,-3
CM,_Y1,AREA	/GO
CHKMSH,'AREA'	DL,P51X, ,UZ,
CMSEL,S,_Y	FLST,2,3,4,ORDE,2
AMESH,_Y1	FITEM,2,1
CMDELE,_Y	FITEM,2,-3
CMDELE,_Y1	/GO
CMDELE,_Y2	DL,P51X, ,ROTX,
CMSEL,S,SABIT_DIE	FLST,2,3,4,ORDE,2
FLST,5,8,5,ORDE,2	FITEM,2,1
FITEM,5,12	FITEM,2,-3
FITEM,5,-19	/GO
CM,_Y,AREA	DL,P51X, ,ROTY,
ASEL, , , ,P51X	FLST,2,3,4,ORDE,2
CM,_Y1,AREA	FITEM,2,1
CMSEL,S,_Y	FITEM,2,-3
CMSEL,S,_Y1	/GO
AATT, 3, 3, 3, 0,	DL,P51X, ,ROTZ,
CMSEL,S,_Y	*DEL,in1
CMDELE,_Y	*DEL,in1
CMDELE,_Y1	*DIM,in1, ,6
FLST,5,8,5,ORDE,2	*SET,in1(1),4.847,-2.416,0,2.942,0,7.771
FITEM,5,12	EDIPART,2,ADD, ,0.28455e-3,0,in1
FITEM,5,-19	FINISH
CM,_Y,AREA	/SOL
ASEL, , , ,P51X	TIME,1,

APPENDIX B

SAMPLE SHEET METAL BENDING SIMULATION RESULTS

For a material having E = 70,000 MPa, σ_{yield} = 180 MPa, R_b = 25 mm and thickness of 1 and 2 mm, sheet metal bending simulations are prepared as shown in Figure B.1.

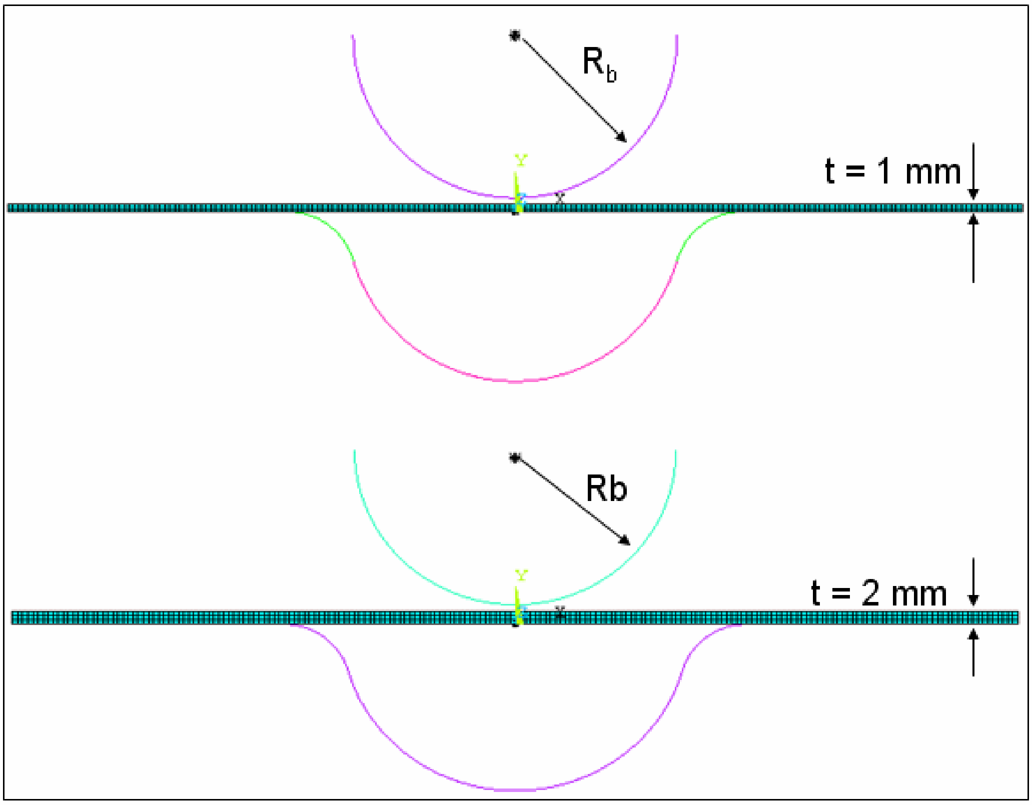

Figure B.1 Finite Element Model of Sheet Metal Bending Operation

According to analytical results as given below, springback angles are calculated for these particular cases, and they are compared with finite element analysis results. In conclusion, when thickness increases, springback angle decreases.

$$\frac{R_b}{R_f} = 1 - 3\cdot\left(\frac{R_b}{h}\cdot\frac{Y}{E}\right) + 4\cdot\left(\frac{R_b}{h}\cdot\frac{Y}{E}\right)^3 \tag{B.1}$$

$$\alpha_f = \left(\frac{R_b + \frac{h}{2}}{R_f + \frac{h}{2}}\right)\cdot\alpha_b \tag{B.2}$$

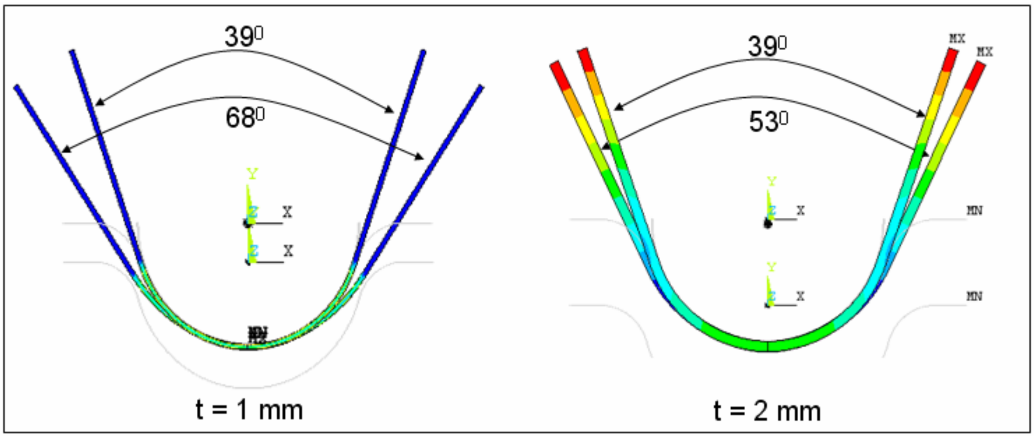

Figure B.2 Finite Element Analysis Results

For t = 1 mm, analytical result gives 27^0 springback angle, whereas FEA result gives 29^0. For t = 2 mm, analytical result gives 13^0 springback angle, whereas FEA result gives 14^0 as shown in Figure B.2.